The evolutionary history and modern diversity of triterpenoid cyclases

Hanon McShea[1], Robb A. Viens[1], Babatunde O. Olagunju[2], José-Luis Giner[2], and Paula V. Welander[1*]

[1]*Department of Earth System Science, Stanford University, Stanford, CA, USA*

[2]*Department of Chemistry, SUNY-ESF, Syracuse, NY, USA*

*Correspondence: Paula Welander welander@stanford.edu

Abstract

Cyclic terpenoids are a class of lipid compounds containing immense structural and functional diversity, with many cyclic triterpenoids acting as membrane components, and, for a few well-studied molecules, regulators of membrane physical properties and spatial organization. Cyclic terpenoids are also readily preserved as terpane fossils, such as steranes and hopanes, which form a rich record of the evolution of life on Earth. Formation of the multiple ring structure of all cyclic terpenoids is catalyzed by terpenoid cyclase enzymes, among which are whole clades of proteins – many from environmental metagenomes and uncultured organisms – whose substrates and products are completely unknown. We investigate the function of these divergent cyclases through biochemical assays, and the evolutionary processes that produced them by testing and applying a variety of evolutionary models. We find a deep divergence between the diterpenoid cyclases and all other cyclases. This roots the triterpenoid cyclase tree, demonstrating reciprocal monophyly between squalene-hopene cyclases and sterol cyclases, which is consistent with their simultaneous first occurrence in the geological record. Through a simple test of evolutionary rate shifts, we find positive selection on the enzyme active site on the squalene-hopene cyclase stem. Finally, by testing the activity of divergent cyclases for a variety of substrates, we find a group of stem sterol cyclases from bacteria that synthesize arborinols, two of which produce the molecular precursor to a Permian "orphan biomarker." Together, our data present an evolutionary framework for triterpenoid cyclases that can inform both the biochemical potential of these proteins and their products' occurrence in the geological record.

Introduction

In 1971, "geohopanes" were discovered in vast quantities in organic-rich sediments, ancient rocks, and fuel reservoirs (Ourisson & Albrecht, 1992). In the following years, hopanoid molecules from diverse bacteria were identified as the biological source of these molecular fossils (Förster et al., 1973; Ourisson & Rohmer, 1992). The finding precipitated a new era of research on the taxonomic distribution and physiological function of cyclic triterpenoids (hopanoids, sterols, and similar molecules shown in Figure 1A) and the triterpenoid cyclase enzymes that synthesize them, motivated by questions of what the molecular fossil record could reveal about the evolution of life on Earth, and of Earth itself (e.g. Fischer, 2008; Ourisson & Nakatani, 1994; Runnegar, 1991; Schaeffer et al., 1994). This body of research has uncovered diverse triterpane fossils, as well as an increasingly deep understanding of the modern structural diversity (Hayashi et al., 2007; Kontnik et al., 2008; Moosmann et al., 2020; Rudolf et al., 2021), taxonomic distribution (Mayer et al., 2021; Pearson et al., 2003; Ricci et al., 2014; Takishita et al., 2017; Villanueva et al., 2014, p. 201; Wei et al., 2016), biosynthesis (Banta et al., 2015; Brown et al., 2023; Lee et al., 2018, 2023; J.-J. Pan et al., 2015; Pollier et al., 2019; Welander et al., 2010), and function (Brenac et al., 2019; Flesch & Rohmer, 1987; Gudde et al., 2019; Rivas-Marin et al., 2019; Schmerk et al., 2015; Welander et al., 2009, 2012; Welander & Summons, 2012; Zhai et al., 2023) of cyclic terpenoid molecules. Unsurprisingly, the catalogues of triterpane fossils and modern triterpenoid diversity are not isomorphic – there are many "orphan biomarkers" in the geological record with no known biological source (Brocks & Pearson, 2005), and conversely, there are many organisms and environments that have genes for triterpenoid cyclases, but no known biosynthetic products (Pearson et al., 2007). To reconcile such orphan

biomarkers and mystery cyclases, we analyzed the modern diversity and evolutionary history of the terpenoid cyclase protein superfamily, of which triterpenoid cyclases are one protein family.

Terpenoid cyclases rearrange carbon-carbon bonds to form polycyclic molecules through an exquisitely precise carbocation cascade (Abe et al., 2014; Eschenmoser & Arigoni, 2005; T. Hoshino & Sato, 2002). We refer here specifically to the Type II terpenoid cyclase protein family, which protonates substrates with a general acid, and is distinct from the Type I terpenoid cyclase family, which adopts a different fold and employs a different, metal-dependent mechanism to cyclize C_{10}, C_{15}, and C_{20} substrates (Christianson, 2017). Type II terpenoid cyclases typically have a dumbbell shape composed of two homologous structural domains known as the β and γ domains. The enzyme substrate pocket is between the two domains, accessible by a substrate channel through the γ domain, while the β domain has a catalytic aspartic acid, and a water tunnel needed to replenish it. Some Type II cyclases have additional domains or lack the γ domain. All domains share the α-α toroid fold, which is a ring of 12 α helices arranged in two concentric rings of 6 (Figure 1). As described by the Structural Classification of Proteins 2.08 (Chandonia et al., 2022; Fox et al., 2014), terpenoid cyclases and protein prenyltransferases make up one of the six superfamilies in the α-α toroid fold, the others being glycosidases, polysaccharide lyases, an enzyme involved in the synthesis of lanthipeptide antibiotics (Zhang et al., 2012), and eukaryotic α2-macroglobulins and complement proteins (Cao et al., 2010).

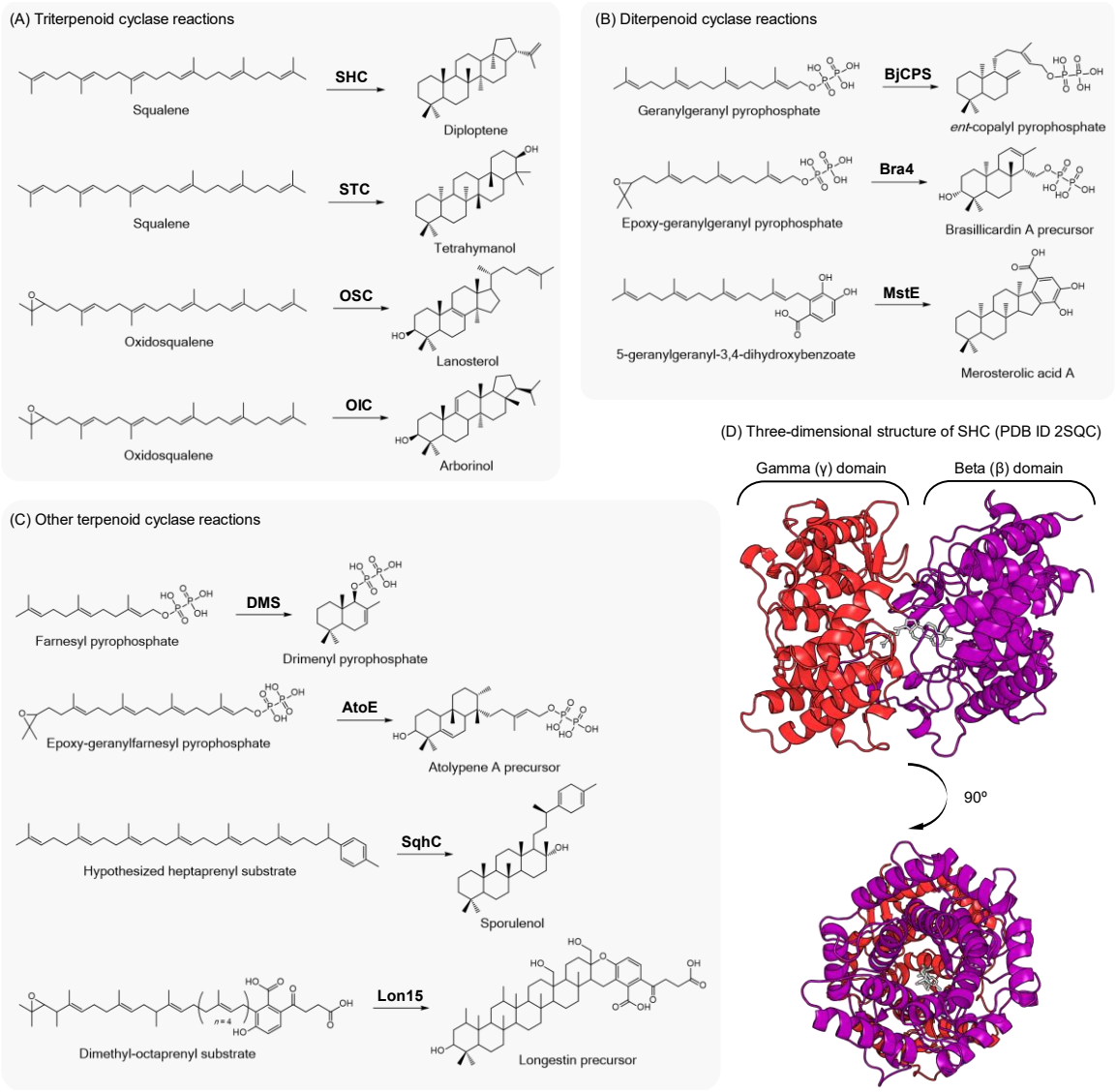

Figure 1: Reactions performed by Type II terpenoid cyclases, including on (A) C_{30} substrates in the case of triterpenoid cyclases, (B) C_{20} substrates in the case of diterpenoid cyclases, and (C) C_{15}, C_{25}, C_{35}, and C_{40} substrates for other Type II terpenoid cyclases. Other reactions exist for some substrates; for example, in addition to lanosterol cyclases, there are oxidosqualene cyclases that synthesize parkeol, cycloartenol, or amyrins. (D) The crystal structure of squalene-hopene cyclase from *Alicyclobacillus acidocaldarius* (Wendt et al., 1999). SHC: squalene-hopene cyclase; STC: tetrahymanol cyclase; OSC: oxidosqualene cyclase; OIC: oxidosqualene-isoarborinol cyclase; BjCPS: *Bradyrhizobium japonicum* copalyl diphosphate synthase; Bra4: brasilicardin cyclase; MstE: merosterolic acid synthase; DMS: drimenol synthase; AtoE: atolypene synthase; SqhC: sporulenol synthase; Lon15: terpene cyclase (longestin).

Type II terpenoid cyclases include triterpenoid (C_{30} substrate) and diterpenoid (C_{20} substrate) cyclases, which share a catalytic mechanism and βγ domain architecture (Christianson, 2017). Triterpenoid cyclases include oxidosqualene cyclases, which cyclize an epoxidized substrate to form molecules such as lanosterol, parkeol, cycloartenol, arborinols, and amyrins (R. Xu et al., 2004). Squalene-hopene cyclases and tetrahymanol cyclases cyclize squalene to form hopenes, and tetrahymanol, respectively. Diterpenoid cyclases cyclize geranylgeranyl pyrophosphate (C_{20}) to form bicyclic copalyl (Ikeda et al., 2007; Morrone et al., 2009; Smanski et al., 2011), halimadienyl (Nakano et al., 2005), terpentedienyl (Dairi et al., 2001; Stowell et al., 2022), and kolavenyl (Nakano et al., 2015) diphosphates, among other molecules. Other diterpenoid cyclases work on epoxidized geranylgeranyl pyrophosphate, forming tricyclic molecules such as brasilicardin (Hayashi et al., 2008), phenalinolactone (Dürr et al., 2006), and tiancilactone (L.-B. Dong et al., 2018) precursors. As shown in Figure 1, the protein family includes the above and also C_{15} (X. Pan et al., 2022; Vo et al., 2022), C_{25} (Kim et al., 2019), C_{35} (Kontnik et al., 2008; Sato, Hoshino, et al., 2011; Sato, Yoshida, et al., 2011), and C_{40} (Hayashi et al., 2007; Ozaki et al., 2018) cyclases, which work on a variety of alkenyl, epoxidized, and otherwise functionalized isoprenoid substrates.

Products of triterpenoid cyclases often undergo modification by other enzymes and go on to regulate membrane homeostasis and dynamics, among other functions (Bloch, 1983). The best-studied example is cholesterol in the animal cell membrane, where it buffers membrane flexibility against temperature changes (Crockett, 1998; Mouritsen & Zuckermann, 2004) and organizes the membrane into liquid-ordered microdomains (Levental et al., 2020; X. Xu & London, 2000). There is evidence for similar function for hopanoids in bacteria (López & Kolter,

2010; Sáenz, 2010; Sáenz et al., 2012, 2015). Cyclic diterpenoids, on the other hand, are commonly modified with solubilizing functional groups after cyclization, and function in cell-cell and interspecific communication. Diterpenoids cyclized by Type I cyclases, on the other hand, are often insoluble and are involved in other functions such as plant wound healing in the form of resins. Other well-studied diterpenoids include the gibberellin hormones made by plants and their symbionts to regulate tissue growth (Nett et al., 2022). Cyclic diterpenoids are also involved in interspecies conflict – between microbes in the form of antibiotics such as terpentecin (Tamamura et al., 1985), platencin (Jayasuriya et al., 2007; Wang et al., 2007), platensimycin (Wang et al., 2006), and phenalinolactone (Gebhardt et al., 2011), antifungals such as viguiepinol and oxaloterpins (Bi & Yu, 2016), and between humans and their pathogens in the case of tuberculosinol from *Mycobacterium tuberculosis* (Mann et al., 2009) and brasilicardin A from *Nocardia brasiliensis* (Shigemori et al., 1998; Usui et al., 2006).

The evolutionary processes that generated the structural and functional diversity of terpenoids have been a subject of great scientific interest (Bloch, 1983; Ourisson, 1989; Ourisson & Nakatani, 1994). Fischer and Pearson (2007) presented several alternative models for relationships among triterpenoid cyclases under parsimonious evolution of three functional traits, which they posit evolve independently and slowly, if not irreversibly: substrate (squalene vs. oxidosqualene), reaction favorability (number of anti-Markovnikov carbocations propagated during the reaction), and product stereochemistry (whether the first three rings are chair-chair-chair vs. chair-boat-chair). In this study, we adopt their rigorous evolutionary approach and update it with four new sources of information, in pursuit of the same biological question: in what order, and through what processes, did the diversity of polycyclic membrane regulators arise?

We first apply a probabilistic method (maximum likelihood) of estimating relationships among cyclases, using an explicit model of protein sequence evolution. This allows us to relax Fischer and Pearson's (2007) assumptions about the independence of the traits and the (slow) speed at which they evolve. Therefore, we can observe the distribution of the selected cyclase traits across a tree generated under unrelated assumptions rather than using these trait assumptions to build the tree. We also revise the list of traits based on functional studies of cyclases over the past 16 years. Our use of probabilistic phylogenetic methods follows that of previous workers (Desmond & Gribaldo, 2010; Frickey & Kannenberg, 2009; Gold et al., 2017; Santana-Molina et al., 2020), and we find that our analyses, where they overlap, recapitulate theirs. Second, we analyze the astounding cyclase diversity sequenced in the intervening 16 years, with special attention to divergent cyclase sequences from environmental metagenomes and metagenome-assembled genomes as a potential source of cyclases that synthesize orphan biomarkers or novel natural products. Previous environmental sequencing efforts focused on triterpenoid cyclases found entire clades comprised solely of metagenomic sequences (Pearson et al., 2007; Pearson & Rusch, 2009), all of which remain uncharacterized. Third, we broaden the analysis to include homologous proteins that work on different substrates, including diterpenoid cyclases and other enzymes that cyclize terpenoid substrates, as well as more distantly related homologs. Putting the triterpenoid cyclase protein family in the evolutionary context of the larger superfamily and fold to which it belongs allows us to root the triterpenoid cyclase tree, again independently of assumptions about the manner in which functional traits evolve. Fourth and finally, using the evolutionary framework provided by an explicit model of protein evolution, sequence diversity, and the α-α toroid fold, we identify cyclases that branch at key transitions in the family's evolution. We test the function of these cyclases via heterologous expression in

Escherichia coli and find two surprising enzymes. One is a cyclase that synthesizes isoarborinol, an orphan biomarker from the Paleozoic. The other is a group of putative squalene-hopene cyclases which cyclize oxidosqualene (the native sterol cyclase substrate) but not squalene (the native squalene-hopene cyclase substrate). In addition to other lines of evidence, the substrate specificity of these cyclases suggests that alkenyl substrates may not be ancestral to triterpenoid cyclases, and were gained relatively late in the squalene-hopene cyclase lineage.

Results and Discussion

Phylogeny

We began our analyses of cyclase evolution by estimating the phylogeny of all proteins known to share the cyclase fold, including triterpenoid, diterpenoid, and meroterpenoid cyclases, and cyclase homologs of unknown function from environmental metagenomes (Figure 2). To do so, we retrieved cyclase homologs from public databases using BLAST and Pfam-based methods (see Material and Methods). Combined, these searches resulted in 44,209 unique sequences after removing duplicates and filtering for length. Briefly, all sequences in this database were aligned, alignments were subset to 1,139 sequences, and phylogenetic trees were estimated under maximum likelihood. To our knowledge this is the first phylogenetic analysis to incorporate a wide diversity of both di- and tri-terpenoid cyclases.

We tested the robustness of tree topology to uncertainty in alignment, model choice, and history of domain duplication and loss. Figure 2 shows the cyclase phylogeny estimated under EX_EHO+R5, which applies separate evolutionary models to each site depending on its probability of being on the protein's surface or buried, and depending on whether it is in an α helix, a loop, or another structural element (Le & Gascuel, 2010). This model also calculates the

probability of each site being in one of 5 evolutionary rate categories. While the distribution of these categories differed slightly between the β and γ domains, we found that the likelihood-maximizing partitioning scheme for the concatenation of domains was a single partition. The topology estimated under EX_EHO+R5 is robust to omission of γ domains, to alignment masking, to larger and smaller subsets of the sequence database, and to model misspecification, as the same deep splits were recovered under runner-up models (Supplementary Table 2). However, ultrafast bootstrap support improved dramatically under better-fitting models.

The domain structure of all cyclases in this tree is either β, βγ, βx, or αβγ. We noticed that β and γ domains crystal structures do not align well, despite clear secondary structural and topological homology (Supplementary Table 1). This could be because they arose from independent duplications of the β domain. If so, the diterpenoid and triterpenoid cyclase γ domains would still be homologous but could have arisen from β domains with different sequences, in different organisms, resulting in different trajectories through fitness landscapes and resultingly independent evolutionary constraints, rates, and substitution processes. For this reason, we used structural alignments of protein crystals to create custom hidden Markov models (HMMs) for the β domain, the diterpenoid cyclase γ domain, and the triterpenoid cyclase γ domain. Our triterpenoid γ domain HMM did not pick up the diterpenoid γ domain, and vice versa. We estimated cyclase phylogeny with the two γ domains aligned separately and recovered the same topology as when γ domains were aligned together, or omitted.

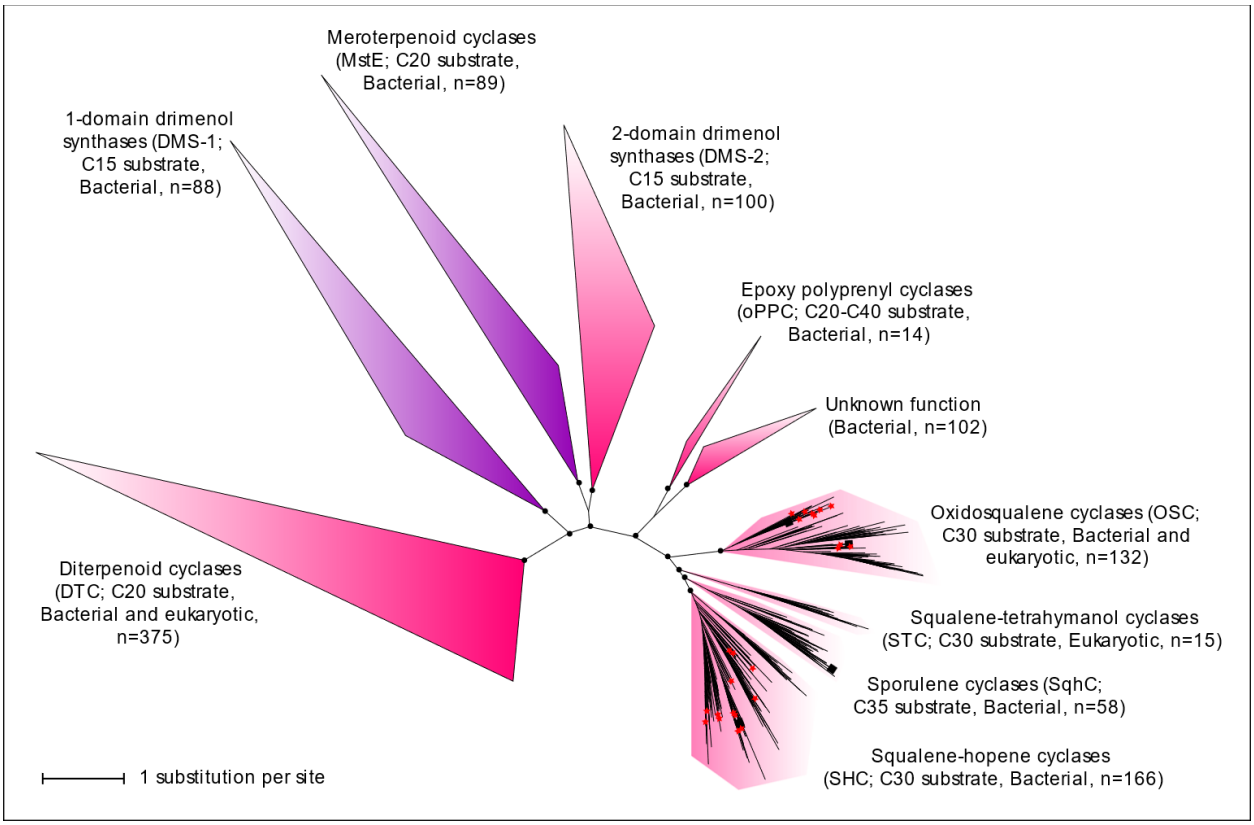

Figure 2: Maximum-likelihood phylogeny of terpenoid cyclases estimated under the EX_EHO model with 5 free rate categories. Stars indicate cyclases from environmental metagenomes; black squares indicate cyclases of known function. Ultrafast bootstrap support is shown for deep splits, where black circles indicate bootstrap ≥ 97.

Major clades

The overall tree topology is consistent with previously published triterpenoid and diterpenoid subtrees (Desmond & Gribaldo, 2010; Frickey & Kannenberg, 2009; Gold et al., 2017; Santana-Molina et al., 2020), and with a tree of all terpenoid cyclases recently published in a review article (Y. Hoshino & Villanueva, 2023). Squalene-hopene cyclases (SHCs) and oxidosqualene cyclases (OSCs) form monophyletic sister clades, with squalene-tetrahymanol cyclases (STCs) from microbial eukaryotes and sporulenol synthases (SqhCs) from Firmicutes forming small groups on the SHC stem, and bacterial OSC groups on the OSC stem.

Sister to this mostly-triterpenoid group is another pair of clades, one of which is a small group of epoxy-polyprenyl cyclases. These enzymes take a substrate that is epoxidized like oxidosqualene but has all head-tail joined isoprene units rather than the central tail-tail linkage of squalene (Figure 1). The epoxy-polyprenyl cyclases include Lon15, a meroterpenoid octaprenyl (C_{40}) cyclase from Actinomycete *Streptomyces argenteolus* (Hayashi et al., 2007) and AtoE, a unique C_{25} cyclase from Actinomycete *Amycolatopsis tolypomycina* NRRL B-24205 (Kim et al., 2019). Most sequences in this clade are from Actinomycetes, with a handful from Chloroflexota and Clostridia. Surprisingly, those diterpenoid cyclases that utilize an epoxidized substrate – Bra4 and PlaT2, epoxy-diterpenoid cyclases from *Nocardia brasiliensis* IFM 0406 (Hayashi et al., 2008) and *Streptomyces* sp. Tu¨ 6071 (Dürr et al., 2006), respectively – also fall in this clade rather than with other diterpenoid cyclases. It seems that the deepest split in the terpenoid cyclase tree is not between diterpenoid and triterpenoid cyclases as we hypothesized but between those that use a substrate with a fully alkenyl isoprenoid chain and those that use an epoxidized substrate – making the alkenyl substrates of the SHC/STC/SqhC clade an independent evolution of that trait from an epoxy ancestor.

Sister to the epoxy-polyprenyl cyclase group is a clade of unknown function referred to in the literature (e.g., Santana-Molina et al., 2020) as “SHC-like.” This clade contains sequences from the PVC group (Planctomycetes, Verrucomicrobia, Chlamydiae), the FCB group (Fibrobacterota, Chlorobiota, Bacteroidota), Spirochaetota, and Acidobacteriota. The function of these proteins, including those from cultured and genetically tractable organisms such as *Gemmata obscuriglobus*, has not been demonstrated, and their molecular structure has not been determined. However, we found that for both groups, the γ domains match only the custom “triterpenoid” γ domain HMM we generated but not our “diterpenoid” γ domain HMM. This

could be due to functional divergence of the γ domains in these two halves of the tree (see "evolutionary implications" below).

On the tree's central long branch is a large clade with three subgroups. One is composed of monodomain (β-only) meroterpenoid cyclases located on the central long branch of the cyclase tree, including a single characterized enzyme called MstE. This cyclase from Cyanobacterium *Scytonema sp.* PCC 10023 cyclizes a quinone precursor with a functionalized benzyl headgroup and a C_{20} isoprenoid chain (Moosman et al. 2020). Interestingly, MstE protonates an alkenyl substrate with a DxD motif rather than the canonical DxDD motif. Other sequences in this clade are from diverse bacterial taxa, including other Cyanobacteria as well as Alphaproteobacteria, Betaproteobacteria, Gammaproteobacteria, Actinomycetes, Acidobacteriota, Myxococcota, Planctomycetes, Chloroflexi, Bacteroidota, and Bacillota. There are also several archaeal sequences, including from cultured representatives such as *Methanosarcina acetivorans* C2A. The other subgroups in this clade are composed of drimenyl pyrophosphate synthases (DMS), recently discovered enzymes that cyclize a C15 substrate. One contains the two-domain DMS characterized from *Streptomyces showdoensis* (X. Pan et al., 2022), along with homologs from other bacteria, while the other contains the DMS characterized from *Aquimarina spongiae* (Vo et al., 2022), which has only one alpha/alpha toroid domain, fused to a haloacid dehalogenase domain. This clade also contains homologs from actinomycetes, FCB superphylum bacteria, and fungi.

The final major clade consists of diterpenoid cyclases. All characterized proteins in this group take geranylgeranyl pyrophosphate (GGPP) as a substrate. The two most basal clades consist of only bacterial proteins, including a characterized bacterial cyclase that makes the gibberellin precursor *ent*-copalyl pyrophosphate. This is sister to a pair of clades containing

fungal *ent*-copalyl pyrophosphate cyclases and plant *ent*-copalyl pyrophosphate cyclases, respectively. The plant clade has many paraphyletic groups of bacterial homologs on its stem, including several characterized enzymes: the *Mycobacterium tuberculosis* cyclase that synthesizes the tuberculosinyl adenosine precursor, the *Kitasatospora griseola* cyclase that synthesizes the terpentecin precursor, and several *ent*-copalyl pyrophosphate cyclases.

Functional analysis of putative metagenomic cyclases

Cyclases from environmental metagenomes are distributed throughout the cyclase tree, especially in bacteria-dominated clades. They fall in the SHC and OSC crown groups, as well as on the stems of these clades, in small groups or as singleton branches. To determine if these metagenomic cyclases are capable of cyclizing squalene or oxidosqualene cyclase, we expressed a select set of cyclases in two strains of *E. coli,* engineered to synthesize squalene or oxidosqualene, respectively, and measured production of polycyclic lipids by gas chromatography-mass spectrometry (GC-MS). We identified 14 triterpenoid cyclase homologs from environmental metagenomes which either branched on the OSC or SHC stem lineage rather than within the crown group or branched within the crown in monophyletic subgroups with no cultured representatives. Many of these cyclases have substitutions at sites of known importance for cyclization of squalene or oxidosqualene.

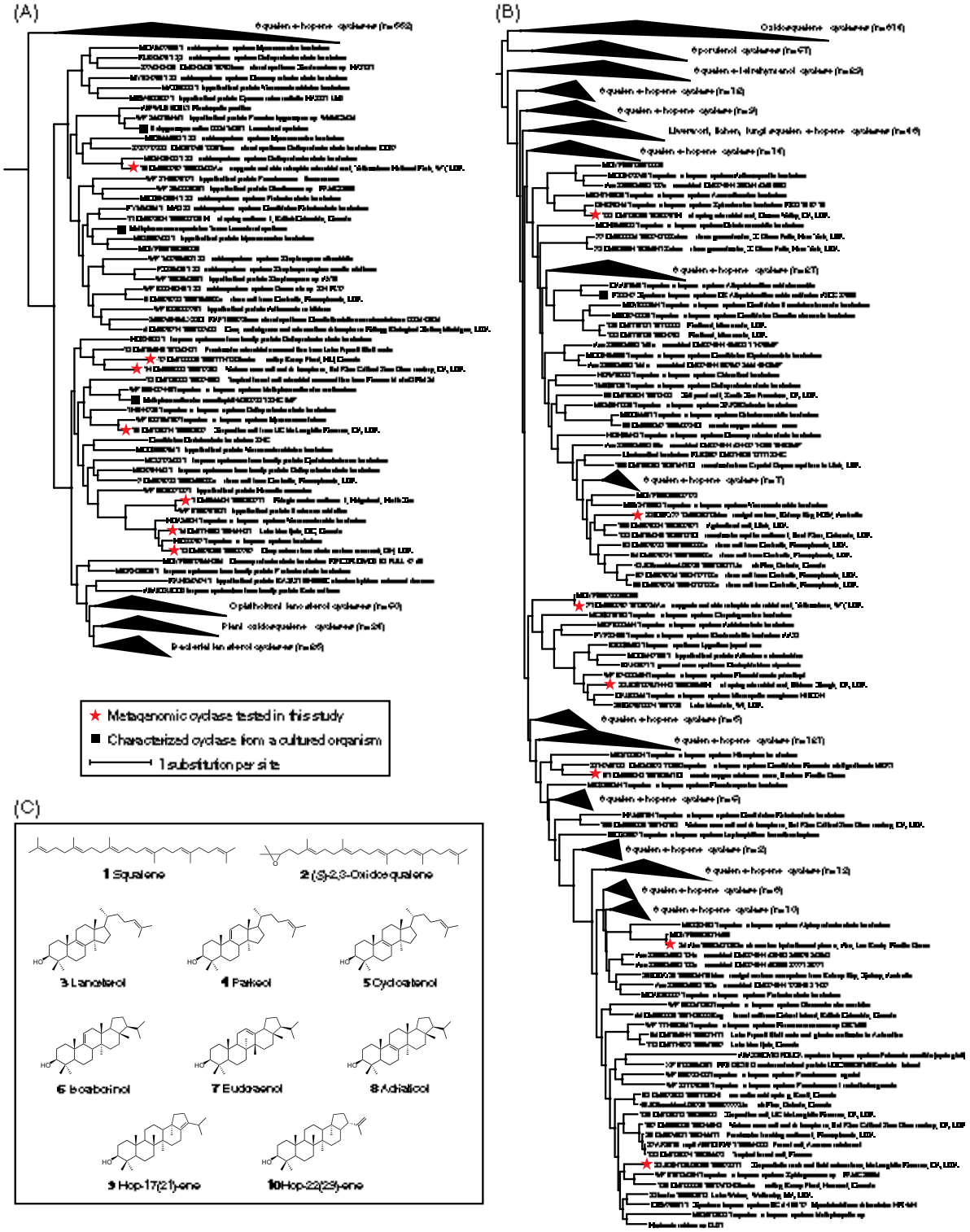

266

267 **Figure 3:** Phylogenetic positions of stem-group triterpenoid cyclases from environmental metagenomes

268 heterologously expressed in *E. coli*. Metagenomic cyclases are marked with red stars, while previously characterized

enzymes from cultured organisms are marked with black squares. (A) Oxidosqualene cyclases. (B) Squalene-hopene cyclases. (C) Substrates and products of cyclases from environmental metagenomes.

Many of the triterpenoid cyclases we selected were active in the heterologous expression system. Most enzymes from the OSC stem produce lanosterol or cycloartenol (Table 1; structures shown in Figure 3C), consistent with their phylogenetic proximity to cyclases from cultured bacteria known to make those products (Figure 3A). No OSC stem cyclases had activity for squalene. One cyclase from a marine metagenome produces eudoraenol, a recently discovered arborane triterpenoid. It is the second eudoraenol-synthesizing enzyme to be reported after the discovery of a eudoraenol cyclase in *Eudoraea adriatica* (Banta et al., 2017), a marine heterotroph from phylum Bacteroidetes (Alain et al., 2008). Close to the eudoraenol cyclases are two cyclases from deep subsurface and inland lake ecosystems which we found synthesize isoarborinol (Figure 4). The subsurface cyclase contig is predicted by the Whokaryote classifier (Pronk & Medema, 2022) to be prokaryotic, making it the first reported bacterial source of isoarborinol. While the lake cyclase contig is too short for classification, its phylogenetic proximity to the subsurface and other bacterial cyclases make it likely to be prokaryotic as well. Arborinol is named for the tree from which it was first isolated (Kennard et al., 1965; Vorbrüggen et al., 1963), but the arborane fossil record stretches back to the Permian (Hauke et al., 1995), well before the evolution of angiosperms, leading to the hypothesis (Ourisson et al., 1982) that microbial sources of arborinols, and specifically isoarborinol, must exist. The formation of isoarborinol by these two cyclases identifies a modern and most likely bacterial source for this “orphan” biomarker. Bacterial arborinol cyclases form a monophyletic clade that diverges from the OSC stem well before the radiation of the OSC crown group, which shows a pattern of vertical inheritance (i.e., major clades of plant, fungal, and animal cyclases largely recapitulate organismal phylogeny). This places the divergence of arborinol cyclases before the

radiation of plants, fungi, and animals, making bacterial arborinol cyclases a very reasonable source for Paleozoic, not to mention Proterozoic, arborane fossils.

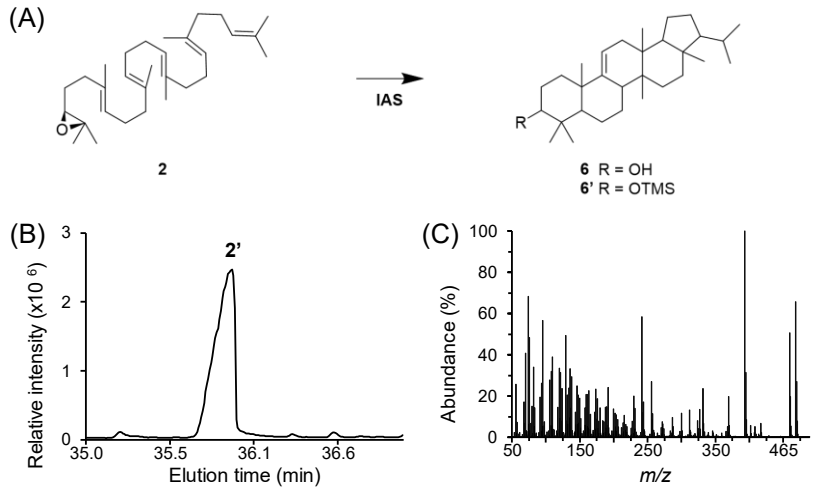

Figure 4: Biosynthesis of isoarborinol by a triterpenoid cyclase from a deep subsurface shale metagenome. (A) The reaction performed by isoarborinol cyclase. (B) GC-MS total ion chromatogram of total lipid extract from *E. coli* strain HM1 expressing the oxidosqualene biosynthesis pathway and Ga0079300_100027797, derivatized to trimethylsilyl (TMS) ethers. (C) Mass spectrum of peak at 36.0 min, identified by comparison to (Vorbrüggen et al., 1963) and by nuclear magnetic resonance (NMR), see Supplementary Figure 3 and Supplementary Table 3.

Most enzymes from the SHC stem (Figure 3B) that we tested produce typical hopene isomers hop-17(21)-ene and/or hop-22(29)-ene from a squalene substrate (Table 1). Hopene-producing enzymes also all had activity for oxidosqualene, typically producing a single hopanol isomer (hopan-22(29)-ol). However, a small group of cyclases within the SHC crown had activity for only oxidosqualene and no activity for squalene, producing only hopanols. This is surprising given that all other cyclases in the SHC clade have some activity for squalene, including sporulenol cyclases, which are functional for both β-curcumene and squalene, and tetrahymanol cyclases. These oxidosqualene cyclases in the SHC clade do not lack any residues

needed to activate squalene. Indeed, they have the electrophilic DxD[D] motif thought to be necessary to protonate an alkenyl substrate. It is possible that these enzymes are in fact true SHCs but cannot cyclize squalene in the *E. coli* cell under the conditions tested, perhaps due to minor protein misfolding that weakens the electrophilicity of the active site, retaining activity for the more reactive substrate but abolishing it for the more recalcitrant one. Indeed, most SHCs tested with oxidosqualene make hopanols (Abe & Rohmer, 1994; Rohmer et al., 1980). It is also possible that these hopanol-producing enzymes are true OSCs in the functional sense, despite being SHCs in the phylogenetic sense, and that substrate functionalization is a relatively labile trait in this group.

Table 1: Substrates and products of triterpenoid cyclases from environmental metagenomes heterologously expressed in *E. coli*. Products were determined by comparison to published GC-MS spectra (see Supplementary Figures 1 and 2), or in the case of isoarborinol, by NMR (Supplementary Figure 3 and Supplementary Table 3).

Cyclase gene ID	Environmental Metagenome	Clade	Substrate	Major products	Strain
Ga0079300_100027797	Deep subsurface shale carbon reservoir, OH, USA	OSC	Oxidosqualene	Isoarborinol	HM1
Ga0123336_1000111412	Glacier valley Borup Fiord, NU, Canada	OSC	Oxidosqualene	Lanosterol	HM3
Ga0114968_100454421	Lake Montjoie, QC, Canada	OSC	Oxidosqualene	Lanosterol, parkeol, adriaticol, isoarborinol	HM4
Ga0055584_1000802711	Pelagic marine sediment, Helgoland, North Sea	OSC	Oxidosqualene	Eudoraenol	HM6
Ga0099828_100017293	Vadose zone soil and rhizosphere, Eel River Critical Zone Observatory, CA, USA	OSC	Oxidosqualene	Cycloartenol	HM23
Ga0126314_100002927	Serpentine soil from UC McLaughlin Reserve, CA, USA	OSC	Oxidosqualene	Cycloartenol	HM31
Ga0068707_100022523	Anoxygenic and chlorotrophic microbial mat, Yellowstone National Park, WY, USA	OSC	Oxidosqualene	Lanosterol, parkeol	HM33
Ga0129299_10203701	Hot spring microbial mat, Owens Valley, CA, USA	SHC	Squalene	Hop-17(21)-ene	RAV2
Ga0068707_10120735	Anoxygenic and chlorotrophic microbial mat, Yellowstone National Park, WY, USA	SHC	Squalene	Hop-17(21)-ene	RAV3
Ga0066848_100168651	Oceanic oxygen minimum zone, Eastern Pacific Ocean	SHC	Squalene	Hop-17(21)-ene	RAV7
JGI11876J14442_100020056	Hot spring microbial mat, Elkhorn Slough, CA, USA	SHC	Squalene	Hop-17(21)-ene	RAV10
BBAY77_1256936218	Macroalgal surface, Botany Bay, NSW, Australia	SHC	Squalene	Hop-17(21)-ene, hop-22(29)-ene	RAV13
Abe_100035313	Black smoker hydrothermal plume, Abe, Lau Basin, Pacific Ocean	SHC	Oxidosqualene (squalene)	Hopanol (no product)	HM163
JGI24120J20309_100072311	Serpentinite rock and fluid subsurface biosphere, McLaughlin Reserve, CA, USA	SHC	Oxidosqualene (squalene)	Hopanol (no product)	HM164

Adaptation in the terpenoid cyclase family

What evolutionary dynamics drove the diversification of terpenoid cyclases? Did their diversity of substrates and products arise from neutral divergence and drift, or did selection play a role? To assess the relative influences of drift and selection, we employed a quantitative test that interprets positive selection as an elevated rate of amino acid mutations in functional regions of the protein structure, along a given branch in a phylogenetic tree (similar to Maddamsetti & Grant, 2022; Ritchie et al., 2021). This approach applies the theory developed for protein-coding nucleotide sequences (e.g. branch-site test, (Gharib & Robinson-Rechavi, 2013; McDonald & Kreitman, 1991; Messer & Petrov, 2013; Yang & Dos Reis, 2011) to protein structures, which allows the test to work on deeply divergent groups where nucleotide substitutions have saturated but structure has evolved more slowly.

Along all the major internal branches of the terpenoid cyclase phylogeny, there are two where a functional domain had a significantly elevated proportion of amino acid substitutions over background (Figure 5). One is the stem of the true SHC clade (that is, the branch between the clade of sporulenol and tetrahymanol cyclases and the SHC crown), where the active site of the protein has an unusually high substitution density. The second is the stem of the group of unknown function, where the SHC-type dimer contact surface had unusually high substitution density. We interpret clustering of substitutions in a functional region as a potential signal of protein adaptation, in which case these may be two instances of positive selective pressure, and/or functional divergence, in the evolutionary history of triterpenoid cyclase homologs. Adaptation could be to new environmental conditions (e.g. to a new host organism after horizontal gene transfer), to new function, or both. That only two instances of positive selection were detectable means either that adaptation on other branches occurred at a molecular length

scale undetectable when focusing on functional regions (e.g. single-residue substitutions), at a temporal scale undetectable when focusing on long branches (e.g. rapid evolution within crown groups), or that the rest of triterpenoid cyclase evolutionary divergence was dominated by drift.

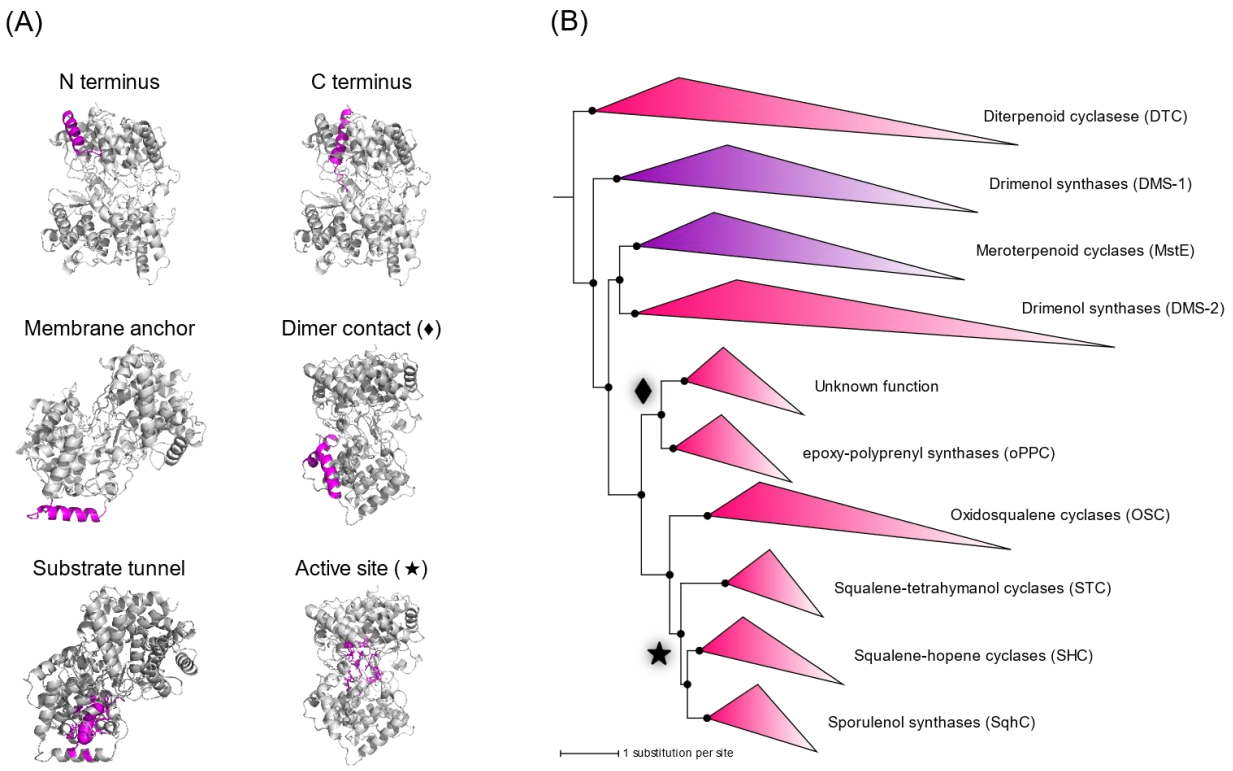

Figure 5: Functionally important domains of triterpenoid cyclases are under positive selection. (A) Functional regions shown on the squalene-hopene cyclase structure (PDB ID 1SQC). Regions found to be under positive selection are marked with a rhombus (♦) and a star (★). (B) Branches with a functional region under positive selection, marked with symbols corresponding to panel A.

Evolutionary Implications

To approach deep splits from another angle, we turn to protein structure, which evolves more slowly than sequence. We applied structural data to estimate relationships in three ways: we used structures to better align sequences before estimating phylogeny under a model of

sequence evolution (Fig 6A), we measured relationships as simple distances between structures (Figure 6B), and we measured relationships using the local structural alphabet implemented in Foldtree (Moi et al., 2023) (Figure 6C).

The structure-aligned sequence tree (Figure 6A) and the RMSD dendrogram (Figure 6B) show a deep split between β domains and γ domains. The β and γ clades have the same internal branching order in the sequence tree, consistent with a single duplication event at the root followed by parallel divergence, with the only other domain rearrangements being the loss of the γ domain in monodomain cyclase 6SBB, gain of the α domain in the ancestor of plant cyclases, and loss of the γ domain later within that clade. The RMSD dendrogram also supports this scenario, and differs only in the relationships among β domains, placing the β domains of bacterial diterpenoid cyclases sister to those of the triterpenoid cyclases rather than those of the plant cyclases. The Foldtree estimate (Figure 6C) predicts a much more complex scenario, with a deep split between plant β domains and the rest of the structures. After the split, the first branches are triterpenoid and sesquiterpenoid γ domains, then tri- and sesqui-terpenoid βs, then diterpenoid βs and γs. This is consistent with our hypothesis of triterpenoid and diterpenoid β domains arising from independent duplication events but suggests a surprising γ domain ancestor for all non-plant β domains. Given that Foldtree does not yet measure statistical support, and given the agreement between the structure-aligned sequence tree, the RMSD dendrogram, and our large sequence-based phylogeny (Figure 2), we tentatively reject the Foldtree estimate and the independent duplications hypothesis. Most evidence supports a single evolution of the terpenoid cyclase γ domain.

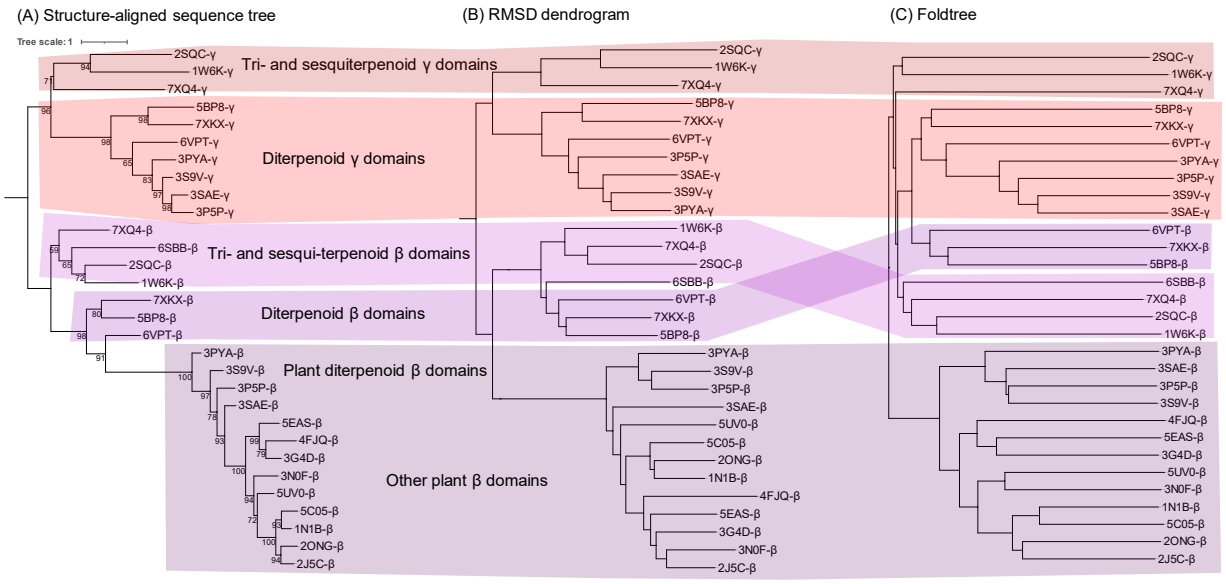

Figure 6: Relationships between cyclase domains estimated using three structure-informed methods. (A) Phylogeny estimated using standard sequence-based method after aligning sequences using structure. (B) Neighbor-joined dendrogram of domains using root mean squared deviation as distances. (C) Structure relationships estimated using the Foldtree algorithm. Red and purple stripes are for visual aid, to show the position of each group across trees.

Given the positive selection on domain structure and substrate functionalization revealed through our structural analyses of these cyclases, we can posit and assess evolutionary scenarios focused on these traits. The longest internal branch of the cyclase phylogeny is between the diterpenoid cyclases and all other proteins (Figure 7A). Rooting the tree on this branch places all-bacterial clades basal to the eukaryotic clades. This is consistent with separate transfer events of diterpenoid cyclases from bacteria to plants and to fungi, likely at different times and involving different donor organisms and proteins. The triterpenoid cyclase root is between the squalene-hopene and oxidosqualene cyclases, consistent with the simultaneous appearance of hopanes and steranes in the rock record (Brocks et al., 2005).

However, rooting on the diterpenoid cyclases implies either three independent evolutions of the γ domain (Figure 7B), or two losses of the γ domain on the MstE and DMS-1 stems (Figure 7C). The first scenario is not supported by the analysis of domain evolution discussed above. The second scenario seems unlikely given that both domains are necessary for function in modern two-domain enzymes, for both substrate positioning and water exclusion (Abe, 2007; Fischer & Pearson, 2007; Wendt, 2005). The unusual cyclase DMS-1 may have had an easier path, with the novel haloacid dehalogenase-like domain (Vo et al., 2022) replacing the γ domain, or inserted between β and γ, in one indel event, never requiring an evolutionary intermediate with a water-exposed active site. On the other hand, the monodomain cyclase merosterolic acid synthase (MstE) excludes water with a mobile loop that caps the active site when substrate is bound (Moosmann et al., 2020). This loop is significantly shorter in the closest related two-domain cyclase, drimenyl diphosphate synthase (X. Pan et al., 2022), suggesting that unless loop extension and domain loss occurred simultaneously, the active site of the MstE ancestor would have been exposed to water, making catalysis impossible.

If we then take domain loss in an MstE ancestor to be less likely than domain loss in a DMS-1 ancestor, a monodomain cyclase root (Figure 7D) becomes worth investigating. Rooting the structure-informed domain tree and the RMSD domain dendrogram on the monodomain cyclase (6SBB) places sesqui- and tri-terpenoid β domains as the next most basal, followed by remaining β domains, from which a monophyletic γ domain clade emerges. Although this position is in all cases far from the tree midpoint, it remains plausible given the evolutionary rarity of domain loss (Bridgham et al., 2009). This scenario best balances that rarity with the evidence for a single origin of the γ domain.

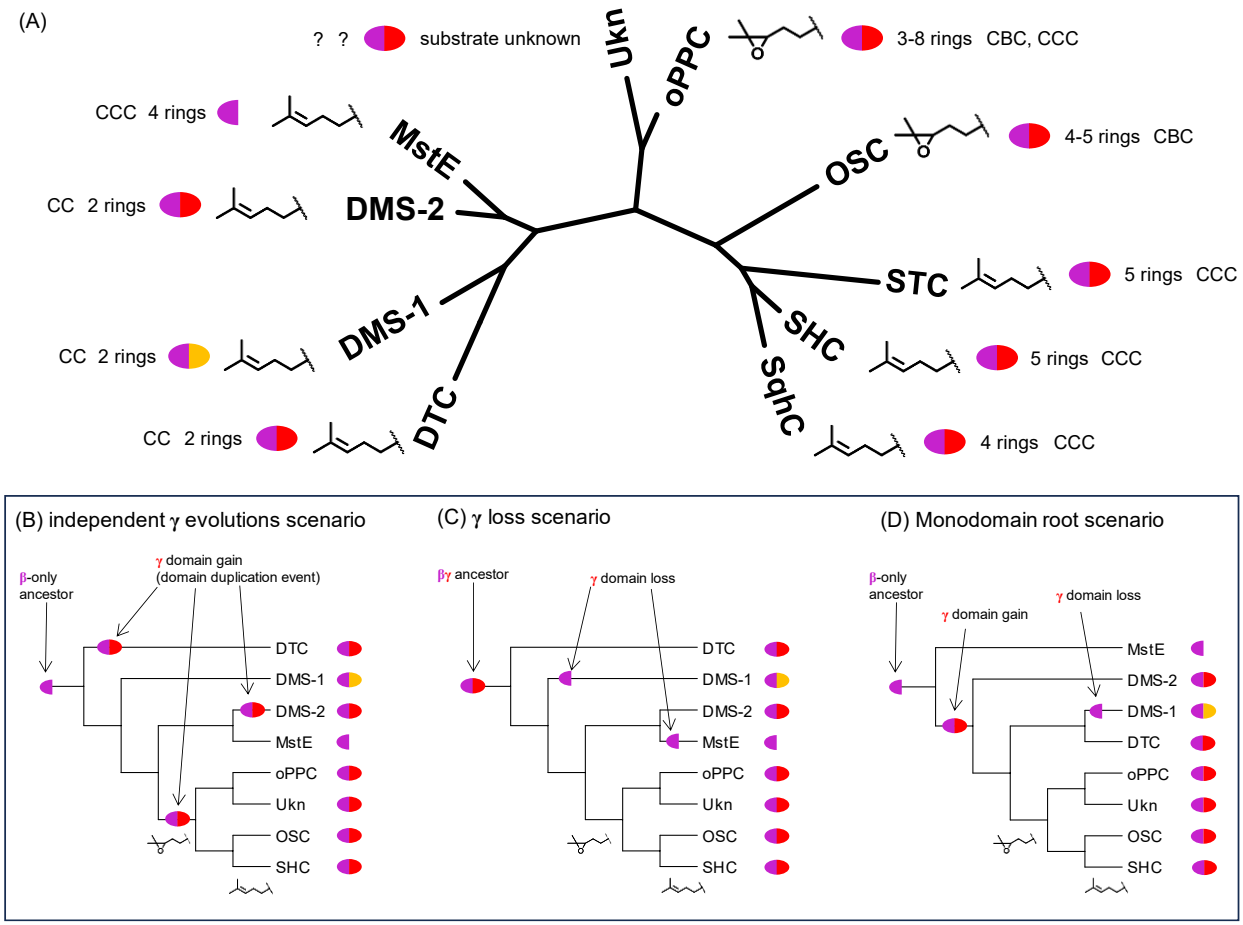

Figure 7: Hypotheses for root position of terpenoid cyclases. (A) Cyclase traits mapped across the unrooted tree, which has the same topology and internal branch lengths as the tree shown in Figure 2. Indicated traits include the number of rings in the final product, the structural conformation of the substrate (CBC: chair-boat-chair or CCC: chair-chair-chair); whether the substrate is epoxidized, and the number of domains (β = purple half-oval, γ = red half-oval, haloacid dehalogenase domain = orange half-oval). This tree is the same as shown in Figures 2 and 3. (B-D) Alternate hypotheses for the root position of the cyclase tree with substrate and domain structure mapped. OSC: oxidosqualene cyclases; SHC: squalene-hopene cyclases; MstE: meroterpenoid cyclases; DTC: diterpenoid cyclases; DMS: drimenyl synthases; Unk: homologs of unknown function; oPPC: oxidopolyprenyl cyclases.

Within the triterpenoid cyclases, the oxidosqualene cyclase clade contains enzymes that form different numbers of rings (4 for sterol cyclases, 5 for arborinol cyclases). The squalene-

hopene cyclases, which form 5 rings, have a stem group comprised of enzymes that form 4 (sporulenol cyclases) or 5 (squalene-tetrahymanol cyclase) rings respectively. Although we have found an outgroup with fewer rings as predicted by Fischer and Pearson (2007), this group also contains an enzyme that forms 8 rings. A gradualist model of evolution, whereby additional rings evolve irreversibly and one-at-a-time, does not fit the data for this trait; rather, the number of rings is relatively labile. This is not surprising since anti-Markovnikov (secondary) carbocations are no longer considered to be cyclization intermediates (Hess, 2002; Hess & Smentek, 2013; J. Tantillo, 2010), removing the physical argument for a teleology of ring number.

Finally, substrate functionalization could have followed two evolutionary paths in the updated phylogeny. Fischer and Pearson (2007) posited that the use of an epoxidized substrate evolved from an alkenyl ancestor once, on the oxidosqualene cyclase stem. In the updated phylogeny, because epoxy-polyprenyl cyclases also used an epoxidized substrate, epoxide use could have evolved twice independently, once in the ancestor of each group. Alternately, it may have evolved once, in the common ancestor of oxidosqualene cyclases and epoxy-polyprenyl cyclases, and subsequently been lost in the squalene-hopene cyclase ancestor. Because alkenyl-substrate enzymes can also cyclize epoxidized substrates, but epoxy-substrate enzymes cannot cyclize alkenyl substrates, evolutionary transitions from alkenyl to epoxy substrates seem in general more likely than the reverse. This is consistent with our discovery of enzymes within the squalene-hopene cyclase crown that only work on an epoxidized substrate (Table 1). The relative probabilities of these two scenarios will be better-informed when the substrate of the “unknown” clade is discovered.

Conclusions

Here we present an updated phylogenetic and functional analysis of triterpenoid cyclases. One result is that the triterpenoid cyclase active site is under positive selection on the SHC stem lineage, perhaps due to adaptation to an alkenyl substrate. Consistent with an ancestral epoxidized substrate is the position of the epoxy-polyprenyl cyclase clade basal to all triterpenoid cyclases. Further, we found possible reversions to an epoxidized substrate in the SHC clade. This experimental result, as well as the discovery of a novel bacterial oxidosqualene-isoarborinol cyclase, show that metagenomic cyclases from uncultured sources are a significant source of diversity and can help inform our understanding of the biochemical potential and evolutionary history of these fascinating enzymes. Future work focused on the functional and structural characterization of these enzymes, particularly those from an uncharacterized clade that branches in the middle of the cyclase tree, will provide invaluable insight that will help constrain the evolutionary scenarios proposed in this study.

Materials and Methods

Gene synthesis and molecular cloning

Cyclase DNA sequences were codon-optimized for expression in *Escherichia coli* and synthesized through the Department of Energy Joint Genome Institute (DOE JGI) DNA Synthesis Science Program. These genes were obtained in the IPTG-inducible plasmid pSRKGm-*lac*UV5-rbs5 (Banta et al., 2017) in *E. coli* TOP10. Plasmid DNA was isolated using the GeneJET Plasmid Miniprep Kit (ThermoFisher Scientific) and sequenced to confirm promoter and gene sequences by ELIM Biopharm (Hayward, CA) using the following primers:

5′-AATGCAGCTGGCACGACAGG-3′ (forward) and 5′-CCAGGGTTTTCCCAGTCAC-3′ (reverse), purchased from Integrated DNA technologies (Coralville, IA).

Bacterial culture and heterologous expression

E. coli DH10B expression strains were transformed by electroporation with the cyclase-bearing pSRKGm plasmid (Khan et al., 2008) and two other plasmids: pJBEI2997 (Addgene plasmid #351515) (Peralta-Yahya et al., 2011) encoding the MEV pathway and a pTrc99a derivative (Amann et al., 1988) encoding squalene synthase (and, in some cases, squalene monooxygenase). Gentamicin (15 μg/mL), carbenicillin (100 μg/mL), and/or chloramphenicol (20 μg/mL) were added to media as appropriate to select for maintenance of each plasmid. Plasmids are described in detail in Supplementary Table 4.

Strains were cultured in 50 mL TYGPN broth (RECIPE) at 37 °C while shaking at 225 rpm. Cultures were induced with 500 μM isopropyl *β*-D-1-thiogalactopyranoside (IPTG) at an OD_{600} of ~0.6, then incubated an additional 48 h at 30 °C while shaking at 225 rpm. Cells were harvested by centrifugation at 4500 × g for 10 min at 4 °C. Cell pellets were stored at −20 °C until lipid extraction. In every experiment, a negative control strain with an empty pSRKgm plasmid and relevant positive controls (strains with pSRKGm containing a triterpenoid cyclase of known function) were grown and extracted alongside experimental strains.

Lipid extraction

Cell pellets were extracted using a modified Bligh–Dyer method (Bligh & Dyer, 1959; Welander et al., 2012): cells were resuspended in 2 mL of deionized water and transferred to a solvent-washed Teflon centrifuge tube containing 5 mL of methanol and 2.5 mL of dichloromethane

(DCM), vortexed for 30 seconds, and sonicated for 1 hour in a water bath sonicator. 10 mL of deionized water and 10 mL of DCM were then added, and samples were vortexed and incubated overnight at −20 °C. Samples were centrifuged for 10 min at 2,800 × g, and the organic layer was transferred to a baked glass vial and evaporated at 40 °C under a gentle stream of N_2 to yield the total lipid extract (TLE). TLE was stored at −20 °C, and derivatized to trimethylsilyl ethers with 1:1 (v:v) bis(trimethylsilyl)trifluoroacetamide (BSTFA):pyridine for 1 h at 70 °C before analysis by gas chromatography–mass spectrometry (GC-MS). The alcohol-soluble fractions of some TLEs were further purified by silicon column chromatography before derivatization, using a solvent series of hexanes, 8:2 hexanes:DCM, DCM, 1:1 DCM:ethyl acetate, and ethyl acetate (Summons et al., 2013).

GC-MS analysis

Lipids were separated with an Agilent 7890B Series GC equipped with two Agilent DB-17HT columns (30 m × 0.25 mm i.d. × 0.15 μm film thickness) in tandem with helium as the carrier gas at a constant flow of 1.1 ml/min and programmed as follows: 100 °C for 2 min, then 12 °C/min to 250 °C and held for 10 min, then 10 °C/min to 330 °C and held for 17.5 min. 2 μL of each sample was injected in splitless mode at 250 °C. The GC was coupled to an Agilent 5977 A Series MSD with the ion source at 230 °C and operated at 70 eV in electron ionization (EI) mode scanning from 50 to 850 Da in 0.5 s. All lipids except isoarborinol were identified based on their retention time and comparison with published spectra. Isoarborinol was identified as a likely sterol by GC-MS, and its structure was confirmed by nuclear magnetic resonance spectroscopy (NMR).

NMR Analysis

NMR experiments were performed following Banta et al. (2017). TLE saponification was accomplished by heating with 10% (vol/vol) sodium hydroxide (NaOH)/MeOH at reflux for 16 h. The reaction mixture was partitioned between water and hexane/ethyl acetate (EtOAc) 2:1; the organic layers were filtered through neutral alumina and concentrated to dryness with a stream of nitrogen. The saponified lipids were fractionated by preparative TLC on glass-backed plates (10 cm in length) coated with a 0.25-mm layer of silica gel 60 F254 using hexane/EtOAc 4:1 as the developing solvent. The triterpenol fraction was further fractionated by reversed-phase HPLC with a system consisting of a Waters 6000A pump, Waters 410 differential refractometer, and two Altex Ultrasphere ODS 5-μm 10 × 250 mm columns in series using a flow rate of 3 mL/min MeOH. After evaporation of the HPLC solvent, the triterpenols were characterized by NMR using a Bruker Avance III HD with an Ascend 800 MHz magnet and a 5-mm TCI cryoprobe at 30 °C using deuterated chloroform (CDCl3) as the solvent. Calibration was by the residual solvent signal (^{1}H: 7.26 ppm; ^{13}C 77.0 ppm).

Sequence search and curation

Cyclase homologs were retrieved from the Joint Genome Institute Integrated Microbial Genomes & Microbiomes database (JGI IMG; https://img.jgi.doe.gov) and the National Center for Biological Informatics nonredundant sequence database (https://www.ncbi.nlm.nih.gov/genbank) using the set of query sequences listed in Supplementary Table 5. Protein-protein BLAST algorithms were used in both cases, with an expect threshold of 0.05 and a word size of 5 for NCBI, and an e-value cutoff of 1e-5 for JGI. Additionally, we downloaded all hits for Pfams PF13243 (squalene-hopene cyclase C-terminal domain) and PF13249 (squalene-hopene cyclase N-terminal domain) from the European Bioinformatics Institute (EBI;

https://www.ebi.ac.uk/interpro/entry/pfam/#table). Combined, these searches resulted in an initial set of 44,209 unique sequences. BLAST results were filtered by length dependent on query sequence as follows: 600-800 amino acids (aa) for triterpenoid cyclases, 550-700 aa for epoxy-polyprenyl cyclases and members of the "unknown function" clade, 700-1,000 aa for plant and fungal diterpenoid cyclases, 450-600 aa for bacterial diterpenoid cyclases, 550-650 aa for DMS1, 450-550 aa for DMS2, and 300-400 aa for MstE. These length ranges were determined based on length distribution of results and length range of functionally characterized representatives of these groups. Sequences from EBI were filtered to a length range of 350 (the length of the smallest known Type II cyclase; Moosmann et al., 2020) to 900 (the length of the largest known Type II domain-bearing cyclase; Mitsuhashi et al., 2017) amino acids. Remaining sequences were subsetted with CD-hit (command cd-hit -i in.fasta -o out.fasta -c 0.90 -n 5 -M 6000 -d 0 -T 8) (Fu et al., 2012) and aligned with the MAFFT v7.402 fftns2 algorithm (Rozewicki et al., 2019), after which sequences lacking an aligned DxD motif were removed (except for oPPC homologs with an [E/D]SA[E/N] motif; Dürr et al., 2006; Hayashi et al., 2008) to yield a database of 13,680 sequences.

Phylogenetic estimation

All sequences in the database described above were aligned using the MAFFT linsi algorithm (Rozewicki et al., 2019) implemented in Magus (Smirnov & Warnow, 2021). The alignment was trimmed using trimAl with a gap threshold of 0.1 (command trimal -in in.aln -out out.aln -gt 0.1), and subsetted with a maximum sequence identity of 50% (command trimal -in in.aln -out out.aln -maxidentity 0.5) (Capella-Gutiérrez et al., 2009). Model selection and maximum likelihood phylogeny estimation were performed with IQ-TREE 2.2.0 (Bui et al., 2020), with the model EX_EHO+R5 (Le & Gascuel, 2010) found to be the best model by Bayesian Information

Criterion and Akaike Information Criterion (Kalyaanamoorthy et al., 2017). For all phylogeny estimation, we performed ≤ 3,000 ultrafast bootstrap replicates (Hoang et al., 2018). All input commands are reported in Supplementary Table 2. Resulting phylogenetic trees were visualized in Dendroscope (Huson & Scornavacca, 2012), Figtree (Rambaut, 2009), or iTOL (Letunic & Bork, 2021).

Structural phylogenetics

We used the rigid-body superposition algorithm mTM-align (R. Dong et al., 2018) to align representative cyclase crystal structures (Supplementary Table 6). To generate the character state matrix, we used this multiple structure alignment to measure and encode every chemical and structural character of the proteins that was both unlikely to be subject to artifacts of crystallization and likely to evolve as slowly or slower than the protein's amino acid sequence: reaction class, active site motif, subunits, loops and helices, and N-terminal tail. The resulting character state matrix became input for Bayesian phylogeny estimation using MrBayes 3.2.6 (Ronquist et al., 2012). We compared these phylogenies to LDDT and TM score trees calculated using a neighbor-joining algorithm implemented in Foldtree (Moi et al., 2023), as well as structural trees calculated using the FoldTree method and sequence trees.

Analysis of adaptation

Using the phylogeny estimated under the model EX_EHO+R5 in IQ-TREE, ancestral protein sequences were reconstructed using IQ-TREE. For each of the branches between major clades (highlighted in Figure 5), most-likely ancestral sequences at the branches' terminal nodes were modeled using ColabFold (Mirdita et al., 2022). We then used Fisher's exact test (2-tail, multiple-test corrected) to measure whether the amino acid substitutions that occurred along that

branch (differences between the two ancestral proteins) are statistically clustered in functional regions of the protein. 6 functional regions were tested: the protein's N terminus, the C terminus, the helix that acts as a membrane anchor, the dimer contact surface, the tunnel from the surface to the active site, and the active site itself (precise region definitions can be found in Supplementary Table 7). Substrate tunnel residues were calculated with Caver (Pavelka et al., 2016) and active site was defined as residues within 5 Å of substrate molecule.

Data availability

The data supporting the findings in this study are available in the main text and supplementary information.

Acknowledgments

The authors would like to thank the students of ESS 143: Molecular Geomicrobiology Lab for hard work and curiosity in initial experiments characterizing the lipid products of several metagenomic triterpenoid cyclases. The authors would like to thank members of the Welander lab, E. Horst, B. Kapili, C.D. Stark, and B. Barros-McShea for critically examining, and thereby improving, this work. We would also like to thank Stanford Research Computing for access to and assistance with the Sherlock High-Performance Computing Environment, where we performed phylogeny estimation and protein structure prediction, and the Stanford Geomicrobiology Shared Laboratories Core Facility (RRID:SCR_025000), where we performed portions of the experimental work. H.M. and P.V.W. were supported by NSF Grant EAR-1752564. H.M. was supported by the National Science Foundation (NSF) Graduate Research Fellowship, the Stanford Enhancing Diversity in Graduate Education (EDGE) Fellowship, and

the Stanford School of Sustainability McGee and Levorsen Graduate Research Grant. R.A.V. was supported by the Stanford Earth Summer Undergraduate Research (SESUR) Program. B.O. and J.L.G. were supported (in part) by National Institutes of Health (NIH) Grant R15GM143714; the 800 MHz NMR was acquired through NIH S10 OD012254.

References

Abe, I. (2007). Enzymatic synthesis of cyclic triterpenes. *Natural Product Reports*, *24*(6), 1311–1331. https://doi.org/10.1039/b616857b

Abe, I., Olano, C., & Carmen, M. (2014). *Evolving Enzymes , Evolving Pathways: The Oxidosqualene Cyclases: One Substrate , Diverse Products Part 1*.

Abe, I., & Rohmer, M. (1994). Enzymic cyclization of 2,3-dihydrosqualene and squalene 2,3-epoxide by squalene cyclases: From pentacyclic to tetracyclic triterpenes. *Journal of the Chemical Society, Perkin Transactions 1*, *0*(7), 783–791. https://doi.org/10.1039/P19940000783

Alain, K., Intertaglia, L., Catala, P., & Lebaron, P. (2008). Eudoraea adriatica gen. Nov., sp. Nov., a novel marine bacterium of the family Flavobacteriaceae. *International Journal of Systematic and Evolutionary Microbiology*, *58*(10), 2275–2281. https://doi.org/10.1099/ijs.0.65446-0

Amann, E., Ochs, B., & Abel, K.-J. (1988). Tightly regulated tac promoter vectors useful for the expression of unfused and fused proteins in Escherichia coli. *Gene*, *69*(2), 301–315. https://doi.org/10.1016/0378-1119(88)90440-4

Banta, A. B., Wei, J. H., Gill, C. C. C., Giner, J.-L., & Welander, P. V. (2017). Synthesis of arborane triterpenols by a bacterial oxidosqualene cyclase. *Proceedings of the National Academy of Sciences*, *114*(2), 245–250. https://doi.org/10.1073/pnas.1617231114

Banta, A. B., Wei, J. H., & Welander, P. V. (2015). A distinct pathway for tetrahymanol synthesis in bacteria. *Proceedings of the National Academy of Sciences*, *112*(44), 13478–13483. https://doi.org/10.1073/pnas.1511482112

Bi, Y., & Yu, Z. (2016). Diterpenoids from Streptomyces sp. SN194 and Their Antifungal Activity against Botrytis cinerea. *Journal of Agricultural and Food Chemistry*, *64*(45), 8525–8529. https://doi.org/10.1021/acs.jafc.6b03645

Bligh, E. G., & Dyer, W. J. (1959). A rapid method of total lipid extraction and purification. *Canadian Journal of Biochemistry and Physiology*, *37*(8), 911–917. https://doi.org/10.1139/o59-099

Bloch, K. E. (1983). Sterol structure and membrane function. *Critical Reviews in Biochemistry and Molecular Biology*, *14*(1), 47–92. https://doi.org/10.3109/10409238309102790

Brenac, L., Baidoo, E. E. K., Keasling, J. D., & Budin, I. (2019). Distinct functional roles for hopanoid composition in the chemical tolerance of Zymomonas mobilis. *Molecular Microbiology*, *112*(5), 1564–1575. https://doi.org/10.1111/mmi.14380

Bridgham, J. T., Ortlund, E. A., & Thornton, J. W. (2009). An epistatic ratchet constrains the direction of glucocorticoid receptor evolution. *Nature*, *461*(7263), 515–519. https://doi.org/10.1038/nature08249

Brocks, J. J., Love, G. D., Summons, R. E., Knoll, A. H., Logan, G. A., & Bowden, S. A. (2005). Biomarker evidence for green and purple sulphur bacteria in a stratified Palaeoproterozoic sea. *Nature*, *437*(7060), 866–870. https://doi.org/10.1038/nature04068

Brocks, J. J., & Pearson, A. (2005). Building the Biomarker Tree of Life. *Reviews in Mineralogy and Geochemistry*, *59*(1), 233–258. https://doi.org/10.2138/rmg.2005.59.10

Brown, M. O., Olagunju, B. O., Giner, J.-L., & Welander, P. V. (2023). Sterol methyltransferases in uncultured bacteria complicate eukaryotic biomarker interpretations. *Nature Communications*, *14*(1), Article 1. https://doi.org/10.1038/s41467-023-37552-3

Bui, M. Q., Schmidt, H. A., Chernomor, O., Schrempf, D., Woodhams, M. D., von Haeseler, A., & Lanfear, R. (2020). IQ-TREE 2: New Models and Efficient Methods for Phylogenetic Inference in the Genomic Era. *Molecular Biology and Evolution*, *37*(5), 1530–1534. https://doi.org/10.1093/molbev/msaa015

Cao, R., Zhang, Y., Mann, F. M., Huang, C., Mukkamala, D., Hudock, M. P., Mead, M. E., Prisic, S., Wang, K., Lin, F.-Y., Chang, T.-K., Peters, R. J., & Oldfield, E. (2010). Diterpene cyclases and the nature of the isoprene fold. *Proteins: Structure, Function, and Bioinformatics*, *78*(11), 2417–2432. https://doi.org/10.1002/prot.22751

Capella-Gutiérrez, S., Silla-Martínez, J. M., & Gabaldón, T. (2009). trimAl: A tool for automated alignment trimming in large-scale phylogenetic analyses. *Bioinformatics*, *25*(15), 1972–1973. https://doi.org/10.1093/bioinformatics/btp348

Chandonia, J.-M., Guan, L., Lin, S., Yu, C., Fox, N. K., & Brenner, S. E. (2022). SCOPe: Improvements to the structural classification of proteins – extended database to facilitate variant interpretation and machine learning. *Nucleic Acids Research*, *50*(D1), D553–D559. https://doi.org/10.1093/nar/gkab1054

671 Christianson, D. W. (2017). Structural and Chemical Biology of Terpenoid Cyclases. *Chemical*
672 *Reviews*, *117*(17), 11570–11648. https://doi.org/10.1021/acs.chemrev.7b00287
673 Crockett, E. L. (1998). Cholesterol Function in Plasma Membranes from Ectotherms:
674 Membrane-Specific Roles in Adaptation to Temperature. *American Zoologist*, *38*(2),
675 291–304. https://doi.org/10.1093/icb/38.2.291
676 Dairi, T., Hamano, Y., Kuzuyama, T., Itoh, N., Furihata, K., & Seto, H. (2001). Eubacterial
677 Diterpene Cyclase Genes Essential for Production of the Isoprenoid Antibiotic
678 Terpentecin. *Journal of Bacteriology*, *183*(20), 6085–6094.
679 https://doi.org/10.1128/JB.183.20.6085-6094.2001
680 Desmond, E., & Gribaldo, S. (2010). Phylogenomics of Sterol Synthesis: Insights into the Origin,
681 Evolution, and Diversity of a Key Eukaryotic Feature. *Genome Biology and Evolution*,
682 *1*(0), 364–381. https://doi.org/10.1093/gbe/evp036
683 Dong, L.-B., Rudolf, J. D., Deng, M.-R., Yan, X., & Shen, B. (2018). Discovery of the
684 Tiancilactone Antibiotics by Genome Mining of Atypical Bacterial Type II Diterpene
685 Synthases. *ChemBioChem*, *19*(16), 1727–1733. https://doi.org/10.1002/cbic.201800285
686 Dong, R., Peng, Z., Zhang, Y., & Yang, J. (2018). mTM-align: An algorithm for fast and accurate
687 multiple protein structure alignment. *Bioinformatics*, *34*(10), 1719–1725.
688 https://doi.org/10.1093/bioinformatics/btx828
689 Dürr, C., Schnell, H.-J., Luzhetskyy, A., Murillo, R., Weber, M., Welzel, K., Vente, A., &
690 Bechthold, A. (2006). Biosynthesis of the terpene phenalinolactone in Streptomyces sp.

Tü6071: Analysis of the gene cluster and generation of derivatives. *Chemistry & Biology*, *13*(4), 365–377. https://doi.org/10.1016/j.chembiol.2006.01.011

Eschenmoser, A., & Arigoni, D. (2005). Revisited after 50 Years: The 'Stereochemical Interpretation of the Biogenetic Isoprene Rule for the Triterpenes.' *Helvetica Chimica Acta*, *88*(12), 3011–3050. https://doi.org/10.1002/hlca.200590245

Fischer, W. W. (2008). Life before the rise of oxygen. *Nature*, *455*(7216), Article 7216. https://doi.org/10.1038/4551051a

Fischer, W. W., & Pearson, A. (2007). Hypotheses for the origin and early evolution of triterpenoid cyclases. *Geobiology*, *5*(1), 19–34. https://doi.org/10.1111/j.1472-4669.2007.00096.x

Flesch, G., & Rohmer, M. (1987). Growth inhibition of hopanoid synthesizing bacteria by squalene cyclase inhibitors. *Archives of Microbiology*, *147*(1), 100–104. https://doi.org/10.1007/BF00492912

Förster, H. J., Biemann, K., Haigh, W. G., Tattrie, N. H., & Colvin, J. R. (1973). The structure of novel C35 pentacyclic terpenes from Acetobacter xylinum. *Biochemical Journal*, *135*(1), 133–143. https://doi.org/10.1042/bj1350133

Fox, N. K., Brenner, S. E., & Chandonia, J.-M. (2014). SCOPe: Structural Classification of Proteins—extended, integrating SCOP and ASTRAL data and classification of new structures. *Nucleic Acids Research*, *42*(D1), D304–D309. https://doi.org/10.1093/nar/gkt1240

Frickey, T., & Kannenberg, E. (2009). Phylogenetic analysis of the triterpene cyclase protein family in prokaryotes and eukaryotes suggests bidirectional lateral gene transfer. *Environmental Microbiology*, *11*(5), 1224–1241. https://doi.org/10.1111/j.1462-2920.2008.01851.x

Fu, L., Niu, B., Zhu, Z., Wu, S., & Li, W. (2012). CD-HIT: Accelerated for clustering the next-generation sequencing data. *Bioinformatics*, *28*(23), 3150–3152. https://doi.org/10.1093/bioinformatics/bts565

Gebhardt, K., Meyer, S. W., Schinko, J., Bringmann, G., Zeeck, A., & Fiedler, H.-P. (2011). Phenalinolactones A–D, terpenoglycoside antibiotics from Streptomyces sp. Tü 6071. *The Journal of Antibiotics*, *64*(3), Article 3. https://doi.org/10.1038/ja.2010.165

Gharib, W. H., & Robinson-Rechavi, M. (2013). The Branch-Site Test of Positive Selection Is Surprisingly Robust but Lacks Power under Synonymous Substitution Saturation and Variation in GC. *Molecular Biology and Evolution*, *30*(7), 1675–1686. https://doi.org/10.1093/molbev/mst062

Gold, D. A., Caron, A., Fournier, G. P., & Summons, R. E. (2017). Paleoproterozoic sterol biosynthesis and the rise of oxygen. *Nature*, *543*(7645), 420–423. https://doi.org/10.1038/nature21412

Gudde, L. R., Hulce, M., Largen, A. H., & Franke, J. D. (2019). Sterol synthesis is essential for viability in the planctomycete bacterium Gemmata obscuriglobus. *FEMS Microbiology Letters*, *366*(3), fnz019. https://doi.org/10.1093/femsle/fnz019

Hauke, V., Adam, P., Trendel, J. M., Albrecht, P., Schwark, L., Vliex, M., Hagemann, H., & Püttmann, W. (1995). Isoarborinol through geological times: Evidence for its presence in the Permian and Triassic. *Organic Geochemistry*, *23*(1), 91–93. https://doi.org/10.1016/0146-6380(95)00002-V

Hayashi, Y., Matsuura, N., Toshima, H., Itoh, N., Ishikawa, J., Mikami, Y., & Dairi, T. (2008). Cloning of the Gene Cluster Responsible for the Biosynthesis of Brasilicardin A, a Unique Diterpenoid. *The Journal of Antibiotics*, *61*(3), Article 3. https://doi.org/10.1038/ja.2008.126

Hayashi, Y., Onaka, H., Itoh, N., Seto, H., & Dairi, T. (2007). Cloning of the Gene Cluster Responsible for Biosynthesis of KS-505a (Longestin), a Unique Tetraterpenoid. *Bioscience, Biotechnology, and Biochemistry*, *71*(12), 3072–3081. https://doi.org/10.1271/bbb.70477

Hess, B. A. (2002). Concomitant C-Ring Expansion and D-Ring Formation in Lanosterol Biosynthesis from Squalene without Violation of Markovnikov's Rule. *Journal of the American Chemical Society*, *124*(35), 10286–10287. https://doi.org/10.1021/ja026850r

Hess, B. A., & Smentek, L. (2013). The Concerted Nature of the Cyclization of Squalene Oxide to the Protosterol Cation. *Angewandte Chemie International Edition*, *52*(42), 11029–11033. https://doi.org/10.1002/anie.201302886

Hoang, D. T., Chernomor, O., von Haeseler, A., Minh, B. Q., & Vinh, L. S. (2018). UFBoot2: Improving the Ultrafast Bootstrap Approximation. *Molecular Biology and Evolution*, *35*(2), 518–522. https://doi.org/10.1093/molbev/msx281

Hoshino, T., & Sato, T. (2002). Squalene – hopene cyclase: Catalytic mechanism and substrate recognition. *Chemical Communications*, *0*(4), 291–301. https://doi.org/10.1039/B108995C

Hoshino, Y., & Villanueva, L. (2023). Four billion years of microbial terpenome evolution. *FEMS Microbiology Reviews*, *47*(2), fuad008. https://doi.org/10.1093/femsre/fuad008

Huson, D. H., & Scornavacca, C. (2012). Dendroscope 3: An Interactive Tool for Rooted Phylogenetic Trees and Networks. *Systematic Biology*, *61*(6), 1061–1067. https://doi.org/10.1093/sysbio/sys062

Ikeda, C., Hayashi, Y., Itoh, N., Seto, H., & Dairi, T. (2007). Functional Analysis of Eubacterial ent -Copalyl Diphosphate Synthase and Pimara-9(11),15-Diene Synthase with Unique Primary Sequences. *The Journal of Biochemistry*, *141*(1), 37–45. https://doi.org/10.1093/jb/mvm004

Jayasuriya, H., Herath, K. B., Zhang, C., Zink, D. L., Basilio, A., Genilloud, O., Diez, M. T., Vicente, F., Gonzalez, I., Salazar, O., Pelaez, F., Cummings, R., Ha, S., Wang, J., & Singh, S. B. (2007). Isolation and Structure of Platencin: A FabH and FabF Dual Inhibitor with Potent Broad-Spectrum Antibiotic Activity. *Angewandte Chemie International Edition*, *46*(25), 4684–4688. https://doi.org/10.1002/anie.200701058

J. Tantillo, D. (2010). The carbocation continuum in terpene biosynthesis—Where are the secondary cations? *Chemical Society Reviews*, *39*(8), 2847–2854. https://doi.org/10.1039/B917107J

Kalyaanamoorthy, S., Minh, B. Q., Wong, T. K. F., von Haeseler, A., & Jermiin, L. S. (2017). ModelFinder: Fast model selection for accurate phylogenetic estimates. *Nature Methods*, *14*(6), Article 6. https://doi.org/10.1038/nmeth.4285

Kennard, O., Riva di Sanseverino, L., Vorbrűggen, H., & Djerassi, C. (1965). The complete structure of the triterpene arborinol. *Tetrahedron Letters*, *6*(39), 3433–3438. https://doi.org/10.1016/S0040-4039(01)89324-2

Khan, S. R., Gaines, J., Roop, R. M., & Farrand, S. K. (2008). Broad-Host-Range Expression Vectors with Tightly Regulated Promoters and Their Use To Examine the Influence of TraR and TraM Expression on Ti Plasmid Quorum Sensing. *Applied and Environmental Microbiology*, *74*(16), 5053–5062. https://doi.org/10.1128/AEM.01098-08

Kim, S.-H., Lu, W., Ahmadi, M. K., Montiel, D., Ternei, M. A., & Brady, S. F. (2019). Atolypenes, Tricyclic Bacterial Sesterterpenes Discovered Using a Multiplexed In Vitro Cas9-TAR Gene Cluster Refactoring Approach. *ACS Synthetic Biology*, *8*(1), 109–118. https://doi.org/10.1021/acssynbio.8b00361

Kontnik, R., Bosak, T., Butcher, R. A., Brocks, J. J., Losick, R., Clardy, J., & Pearson, A. (2008). Sporulenes, heptaprenyl metabolites from Bacillus subtilis spores. *Organic Letters*, *10*(16), 3551–3554. https://doi.org/10.1021/ol801314k

Le, S. Q., & Gascuel, O. (2010). Accounting for Solvent Accessibility and Secondary Structure in Protein Phylogenetics Is Clearly Beneficial. *Systematic Biology*, *59*(3), 277–287. https://doi.org/10.1093/sysbio/syq002

Lee, A. K., Banta, A. B., Wei, J. H., Kiemle, D. J., Feng, J., Giner, J.-L., & Welander, P. V. (2018). C-4 sterol demethylation enzymes distinguish bacterial and eukaryotic sterol synthesis. *Proceedings of the National Academy of Sciences*, *115*(23), 5884–5889. https://doi.org/10.1073/pnas.1802930115

Lee, A. K., Wei, J. H., & Welander, P. V. (2023). De novo cholesterol biosynthesis in bacteria. *Nature Communications*, *14*(1), Article 1. https://doi.org/10.1038/s41467-023-38638-8

Letunic, I., & Bork, P. (2021). Interactive Tree Of Life (iTOL) v5: An online tool for phylogenetic tree display and annotation. *Nucleic Acids Research*, *49*(W1), W293–W296. https://doi.org/10.1093/nar/gkab301

Levental, I., Levental, K. R., & Heberle, F. A. (2020). Lipid Rafts: Controversies Resolved, Mysteries Remain. *Trends in Cell Biology*, *30*(5), 341–353. https://doi.org/10.1016/j.tcb.2020.01.009

López, D., & Kolter, R. (2010). Functional microdomains in bacterial membranes. *Genes & Development*, *24*(17), 893–902. https://doi.org/10.1101/gad.1945010

Maddamsetti, R., & Grant, N. A. (2022). Discovery of positive and purifying selection in metagenomic time series of hypermutator microbial populations. *PLOS Genetics*, *18*(8), e1010324. https://doi.org/10.1371/journal.pgen.1010324

Mann, F. M., Xu, M., Chen, X., Fulton, D. B., Russell, D. G., & Peters, R. J. (2009). Edaxadiene: A New Bioactive Diterpene from Mycobacterium tuberculosis. *Journal of the American Chemical Society*, *131*(48), 17526–17527. https://doi.org/10.1021/ja9019287

Mayer, M. H., Parenteau, M. N., Kempher, M. L., Madigan, M. T., Jahnke, L. L., & Welander, P. V. (2021). Anaerobic 3-methylhopanoid production by an acidophilic photosynthetic purple bacterium. *Archives of Microbiology*, *203*(10), 6041–6052. https://doi.org/10.1007/s00203-021-02561-7

McDonald, J. H., & Kreitman, M. (1991). Adaptive protein evolution at the Adh locus in Drosophila. *Nature*, *351*(6328), Article 6328. https://doi.org/10.1038/351652a0

Messer, P. W., & Petrov, D. A. (2013). Frequent adaptation and the McDonald-Kreitman test. *Proceedings of the National Academy of Sciences*, *110*(21), 8615–8620. https://doi.org/10.1073/pnas.1220835110

Mirdita, M., Schütze, K., Moriwaki, Y., Heo, L., Ovchinnikov, S., & Steinegger, M. (2022). ColabFold: Making protein folding accessible to all. *Nature Methods*, *19*(6), Article 6. https://doi.org/10.1038/s41592-022-01488-1

Mitsuhashi, T., Okada, M., & Abe, I. (2017). Identification of Chimeric αβγ Diterpene Synthases Possessing both Type II Terpene Cyclase and Prenyltransferase Activities. *ChemBioChem*, *18*(21), 2104–2109. https://doi.org/10.1002/cbic.201700445

Moi, D., Bernard, C., Steinegger, M., Nevers, Y., Langleib, M., & Dessimoz, C. (2023). *Structural phylogenetics unravels the evolutionary diversification of communication systems in gram-positive bacteria and their viruses* (p. 2023.09.19.558401). bioRxiv. https://doi.org/10.1101/2023.09.19.558401

Moosmann, P., Ecker, F., Leopold-Messer, S., Cahn, J. K. B., Dieterich, C. L., Groll, M., & Piel, J. (2020). A monodomain class II terpene cyclase assembles complex isoprenoid

833 scaffolds. *Nature Chemistry*, *12*(10), Article 10. https://doi.org/10.1038/s41557-020-
834 0515-3
835 Morrone, D., Chambers, J., Lowry, L., Kim, G., Anterola, A., Bender, K., & Peters, R. J. (2009).
836 Gibberellin biosynthesis in bacteria: Separate ent-copalyl diphosphate and ent-kaurene
837 synthases in Bradyrhizobium japonicum. *FEBS Letters*, *583*(2), 475–480.
838 https://doi.org/10.1016/j.febslet.2008.12.052
839 Mouritsen, O. G., & Zuckermann, M. J. (2004). What's so special about cholesterol? *Lipids*,
840 *39*(11), 1101–1113. https://doi.org/10.1007/s11745-004-1336-x
841 Nakano, C., Okamura, T., Sato, T., Dairi, T., & Hoshino, T. (2005). Mycobacterium tuberculosis
842 H37Rv3377c encodes the diterpene cyclase for producing the halimane skeleton.
843 *Chemical Communications*, *8*, 1016–1018. https://doi.org/10.1039/B415346D
844 Nakano, C., Oshima, M., Kurashima, N., & Hoshino, T. (2015). Identification of a New Diterpene
845 Biosynthetic Gene Cluster that Produces O-Methylkolavelool in Herpetosiphon
846 aurantiacus. *ChemBioChem*, *16*(5), 772–781. https://doi.org/10.1002/cbic.201402652
847 Nett, R. S., Bender, K. S., & Peters, R. J. (2022). Production of the plant hormone gibberellin by
848 rhizobia increases host legume nodule size. *The ISME Journal*, *16*(7), Article 7.
849 https://doi.org/10.1038/s41396-022-01236-5
850 Ourisson, G. (1989). The evolution of terpenes to sterols. *Pure and Applied Chemistry*, *61*(3),
851 345–348. https://doi.org/10.1351/pac198961030345

Ourisson, G., & Albrecht, P. (1992). Hopanoids. 1. Geohopanoids: The most abundant natural products on Earth? *Accounts of Chemical Research*, *25*(9), 398–402. https://doi.org/10.1021/ar00021a003

Ourisson, G., Albrecht, P., & Rohmer, M. (1982). Predictive microbial biochemistry—From molecular fossils to procaryotic membranes. *Trends in Biochemical Sciences*, *7*(7), 236–239. https://doi.org/10.1016/0968-0004(82)90028-7

Ourisson, G., & Nakatani, Y. (1994). The terpenoid theory of the origin of cellular life: The evolution of terpenoids to cholesterol. *Chemistry and Biology*, *1*(1), 11–23. https://doi.org/10.1016/1074-5521(94)90036-1

Ourisson, G., & Rohmer, M. (1992). Hopanoids. 2. Biohopanoids: A novel class of bacterial lipids. *Accounts of Chemical Research*, *25*(9), 403–408. https://doi.org/10.1021/ar00021a004

Ozaki, T., Shinde, S. S., Gao, L., Okuizumi, R., Liu, C., Ogasawara, Y., Lei, X., Dairi, T., Minami, A., & Oikawa, H. (2018). Enzymatic Formation of a Skipped Methyl-Substituted Octaprenyl Side Chain of Longestin (KS-505a): Involvement of Homo-IPP as a Common Extender Unit. *Angewandte Chemie International Edition*, *57*(22), 6629–6632. https://doi.org/10.1002/anie.201802116

Pan, J.-J., Solbiati, J. O., Ramamoorthy, G., Hillerich, B. S., Seidel, R. D., Cronan, J. E., Almo, S. C., & Poulter, C. D. (2015). Biosynthesis of Squalene from Farnesyl Diphosphate in Bacteria: Three Steps Catalyzed by Three Enzymes. *ACS Central Science*, *1*(2), 77–82. https://doi.org/10.1021/acscentsci.5b00115

Pan, X., Du, W., Zhang, X., Lin, X., Li, F.-R., Yang, Q., Wang, H., Rudolf, J. D., Zhang, B., & Dong, L.-B. (2022). Discovery, Structure, and Mechanism of a Class II Sesquiterpene Cyclase. *Journal of the American Chemical Society*, *144*(48), 22067–22074. https://doi.org/10.1021/jacs.2c09412

Pavelka, A., Sebestova, E., Kozlikova, B., Brezovsky, J., Sochor, J., & Damborsky, J. (2016). CAVER: Algorithms for Analyzing Dynamics of Tunnels in Macromolecules. *IEEE/ACM Transactions on Computational Biology and Bioinformatics*, *13*(3), 505–517. IEEE/ACM Transactions on Computational Biology and Bioinformatics. https://doi.org/10.1109/TCBB.2015.2459680

Pearson, A., Budin, M., & Brocks, J. J. (2003). Phylogenetic and biochemical evidence for sterol synthesis in the bacterium Gemmata obscuriglobus. *Proceedings of the National Academy of Sciences*, *100*(26), 15352–15357. https://doi.org/10.1073/pnas.2536559100

Pearson, A., Flood Page, S. R., Jorgenson, T. L., Fischer, W. W., & Higgins, M. B. (2007). Novel hopanoid cyclases from the environment. *Environmental Microbiology*, *9*(9), 2175–2188. https://doi.org/10.1111/j.1462-2920.2007.01331.x

Pearson, A., & Rusch, D. B. (2009). Distribution of microbial terpenoid lipid cyclases in the global ocean metagenome. *The ISME Journal*, *3*(3), 352–363. https://doi.org/10.1038/ismej.2008.116

Peralta-Yahya, P. P., Ouellet, M., Chan, R., Mukhopadhyay, A., Keasling, J. D., & Lee, T. S. (2011). Identification and microbial production of a terpene-based advanced biofuel. *Nature Communications*, *2*(1), Article 1. https://doi.org/10.1038/ncomms1494

Pollier, J., Vancaester, E., Kuzhiumparambil, U., Vickers, C. E., Vandepoele, K., Goossens, A., & Fabris, M. (2019). A widespread alternative squalene epoxidase participates in eukaryote steroid biosynthesis. *Nature Microbiology*, *4*(2), 226–233. https://doi.org/10.1038/s41564-018-0305-5

Pronk, L. J. U., & Medema, M. H. (2022). Whokaryote: Distinguishing eukaryotic and prokaryotic contigs in metagenomes based on gene structure. *Microbial Genomics*, *8*(5), 000823. https://doi.org/10.1099/mgen.0.000823

Rambaut, A. (2009). *FigTree, version 1.4.3*. http://tree.bio.ed.ac.uk/software/Figtree/

Ricci, J. N., Coleman, M. L., Welander, P. V., Sessions, A. L., Summons, R. E., Spear, J. R., & Newman, D. K. (2014). Diverse capacity for 2-methylhopanoid production correlates with a specific ecological niche. *The ISME Journal*, *8*(3), Article 3. https://doi.org/10.1038/ismej.2013.191

Ritchie, A. M., Stark, T. L., & Liberles, D. A. (2021). Inferring the number and position of changes in selective regime in a non-equilibrium mutation-selection framework. *BMC Ecology and Evolution*, *21*(1), 39. https://doi.org/10.1186/s12862-021-01770-4

Rivas-Marin, E., Stettner, S., Gottshall, E. Y., Santana-Molina, C., Helling, M., Basile, F., Ward, N. L., & Devos, D. P. (2019). Essentiality of sterol synthesis genes in the planctomycete bacterium Gemmata obscuriglobus. *Nature Communications*, *10*(1), Article 1. https://doi.org/10.1038/s41467-019-10983-7

Rohmer, M., Anding, C., & Ourisson, G. (1980). Non-specific biosynthesis of hopane triterpenes by a cell-free system from Acetobacter pasteurianum. *European Journal of Biochemistry*, *112*(3), 541–547. https://doi.org/10.1111/j.1432-1033.1980.tb06117.x

Ronquist, F., Teslenko, M., van der Mark, P., Ayres, D. L., Darling, A., Höhna, S., Larget, B., Liu, L., Suchard, M. A., & Huelsenbeck, J. P. (2012). MrBayes 3.2: Efficient Bayesian Phylogenetic Inference and Model Choice Across a Large Model Space. *Systematic Biology*, *61*(3), 539–542. https://doi.org/10.1093/sysbio/sys029

Rozewicki, J., Li, S., Amada, K. M., Standley, D. M., & Katoh, K. (2019). MAFFT-DASH: Integrated protein sequence and structural alignment. *Nucleic Acids Research*, *47*(W1), W5–W10. https://doi.org/10.1093/nar/gkz342

Rudolf, J. D., Alsup, T. A., Xu, B., & Li, Z. (2021). Bacterial terpenome. *Natural Product Reports*, *38*(5), 905–980. https://doi.org/10.1039/D0NP00066C

Runnegar, B. (1991). Precambrian oxygen levels estimated from the biochemistry and physiology of early eukaryotes. *Palaeogeography, Palaeoclimatology, Palaeoecology*, *97*(1), 97–111. https://doi.org/10.1016/0031-0182(91)90186-U

Sáenz, J. P. (2010). Hopanoid enrichment in a detergent resistant membrane fraction of Crocosphaera watsonii: Implications for bacterial lipid raft formation. *Organic Geochemistry*, *41*(8), 853–856. https://doi.org/10.1016/j.orggeochem.2010.05.005

Sáenz, J. P., Grosser, D., Bradley, A. S., Lagny, T. J., Lavrynenko, O., Broda, M., & Simons, K. (2015). Hopanoids as functional analogues of cholesterol in bacterial membranes.

Proceedings of the National Academy of Sciences, *112*(38), 11971–11976. https://doi.org/10.1073/pnas.1515607112

Sáenz, J. P., Sezgin, E., Schwille, P., & Simons, K. (2012). Functional convergence of hopanoids and sterols in membrane ordering. *Proceedings of the National Academy of Sciences*, *109*(35), 14236–14240. https://doi.org/10.1073/pnas.1212141109

Santana-Molina, C., Rivas-Marin, E., Rojas, A. M., & Devos, D. P. (2020). Origin and Evolution of Polycyclic Triterpene Synthesis. *Molecular Biology and Evolution*, *37*(7), 1925–1941. https://doi.org/10.1093/molbev/msaa054

Sato, T., Hoshino, H., Yoshida, S., Nakajima, M., & Hoshino, T. (2011). Bifunctional triterpene/sesquarterpene cyclase: Tetraprenyl-β- curcumene cyclase is also squalene cyclase in bacillus megaterium. *Journal of the American Chemical Society*, *133*(44), 17540–17543. https://doi.org/10.1021/ja2060319

Sato, T., Yoshida, S., Hoshino, H., Tanno, M., Nakajima, M., & Hoshino, T. (2011). Sesquarterpenes (C35 Terpenes) Biosynthesized via the Cyclization of a Linear C35 Isoprenoid by a Tetraprenyl-β-curcumene Synthase and a Tetraprenyl-β-curcumene Cyclase: Identification of a New Terpene Cyclase. *Journal of the American Chemical Society*, *133*(25), 9734–9737. https://doi.org/10.1021/ja203779h

Schaeffer, P., Poinsot, J., Hauke, V., Adam, P., Wehrung, P., Trendel, J.-M., Albrecht, P., Dessort, D., & Connan, J. (1994). Novel Optically Active Hydrocarbons in Sediments: Evidence for an Extensive Biological Cyclization of Higher Regular Polyprenols.

Angewandte Chemie International Edition in English, *33*(11), 1166–1169. https://doi.org/10.1002/anie.199411661

Schmerk, C. L., Welander, P. V., Hamad, M. A., Bain, K. L., Bernards, M. A., Summons, R. E., & Valvano, M. A. (2015). Elucidation of the Burkholderia cenocepacia hopanoid biosynthesis pathway uncovers functions for conserved proteins in hopanoid-producing bacteria. *Environmental Microbiology*, *17*(3), 735–750. https://doi.org/10.1111/1462-2920.12509

Shigemori, H., Komaki, H., Yazawa, K., Mikami, Y., Nemoto, A., Tanaka, Y., Sasaki, T., In, Y., Ishida, T., & Kobayashi, J. (1998). Brasilicardin A. A Novel Tricyclic Metabolite with Potent Immunosuppressive Activity from Actinomycete Nocardia brasiliensis. *The Journal of Organic Chemistry*, *63*(20), 6900–6904. https://doi.org/10.1021/jo9807114

Smanski, M. J., Yu, Z., Casper, J., Lin, S., Peterson, R. M., Chen, Y., Wendt-Pienkowski, E., Rajski, S. R., & Shen, B. (2011). Dedicated ent-kaurene and ent-atiserene synthases for platensimycin and platencin biosynthesis. *Proceedings of the National Academy of Sciences*, *108*(33), 13498–13503. https://doi.org/10.1073/pnas.1106919108

Smirnov, V., & Warnow, T. (2021). MAGUS: Multiple sequence Alignment using Graph clUStering. *Bioinformatics*, *37*(12), 1666–1672. https://doi.org/10.1093/bioinformatics/btaa992

Stowell, E. A., Ehrenberger, M. A., Lin, Y.-L., Chang, C.-Y., & Rudolf, J. D. (2022). Structure-guided product determination of the bacterial type II diterpene synthase Tpn2. *Communications Chemistry*, *5*(1), Article 1. https://doi.org/10.1038/s42004-022-00765-6

Summons, R. E., Bird, L. R., Gillespie, A. L., Pruss, S. B., Roberts, M., & Sessions, A. L. (2013). Lipid biomarkers in ooids from different locations and ages: Evidence for a common bacterial flora. *Geobiology*, *11*(5), 420–436. https://doi.org/10.1111/gbi.12047

Takishita, K., Chikaraishi, Y., Tanifuji, G., Ohkouchi, N., Hashimoto, T., Fujikura, K., & Roger, A. J. (2017). Microbial Eukaryotes that Lack Sterols. *Journal of Eukaryotic Microbiology*, *64*(6), 897–900. https://doi.org/10.1111/jeu.12426

Tamamura, T., Sawa, T., Isshiki, K., Masuda, T., Homma, Y., Iinuma, H., Naganawa, H., Hamada, M., Takeuchi, T., & Umezawa, H. (1985). ISOLATION AND CHARACTERIZATION OF TERPENTECIN, A NEW ANTITUMOR ANTIBIOTIC. *The Journal of Antibiotics*, *38*(12), 1664–1669. https://doi.org/10.7164/antibiotics.38.1664

Usui, T., Nagumo, Y., Watanabe, A., Kubota, T., Komatsu, K., Kobayashi, J., & Osada, H. (2006). Brasilicardin A, a Natural Immunosuppressant, Targets Amino Acid Transport System L. *Chemistry & Biology*, *13*(11), 1153–1160. https://doi.org/10.1016/j.chembiol.2006.09.006

Villanueva, L., Rijpstra, W. I. C., Schouten, S., & Damsté, J. S. S. (2014). Genetic biomarkers of the sterol-biosynthetic pathway in microalgae. *Environmental Microbiology Reports*, *6*(1), 35–44. https://doi.org/10.1111/1758-2229.12106

Vo, N. N. Q., Nomura, Y., Kinugasa, K., Takagi, H., & Takahashi, S. (2022). Identification and Characterization of Bifunctional Drimenol Synthases of Marine Bacterial Origin. *ACS Chemical Biology*, *17*(5), 1226–1238. https://doi.org/10.1021/acschembio.2c00163

Vorbrüggen, H., Pakrashi, S. C., & Djerassi, C. (1963). Terpenoide, LIV. Arborinol, ein neuer Triterpen-Typus. *Justus Liebigs Annalen der Chemie*, *668*(1), 57–76. https://doi.org/10.1002/jlac.19636680107

Wang, J., Kodali, S., Lee, S. H., Galgoci, A., Painter, R., Dorso, K., Racine, F., Motyl, M., Hernandez, L., Tinney, E., Colletti, S. L., Herath, K., Cummings, R., Salazar, O., González, I., Basilio, A., Vicente, F., Genilloud, O., Pelaez, F., … Singh, S. B. (2007). Discovery of platencin, a dual FabF and FabH inhibitor with in vivo antibiotic properties. *Proceedings of the National Academy of Sciences*, *104*(18), 7612–7616. https://doi.org/10.1073/pnas.0700746104

Wang, J., Soisson, S. M., Young, K., Shoop, W., Kodali, S., Galgoci, A., Painter, R., Parthasarathy, G., Tang, Y. S., Cummings, R., Ha, S., Dorso, K., Motyl, M., Jayasuriya, H., Ondeyka, J., Herath, K., Zhang, C., Hernandez, L., Allocco, J., … Singh, S. B. (2006). Platensimycin is a selective FabF inhibitor with potent antibiotic properties. *Nature*, *441*(7091), Article 7091. https://doi.org/10.1038/nature04784

Wei, J. H., Yin, X., & Welander, P. V. (2016). Sterol Synthesis in Diverse Bacteria. *Frontiers in Microbiology*, *7*. https://www.frontiersin.org/articles/10.3389/fmicb.2016.00990

Welander, P. V., Coleman, M. L., Sessions, A. L., Summons, R. E., & Newman, D. K. (2010). Identification of a methylase required for 2-methylhopanoid production and implications for the interpretation of sedimentary hopanes. *Proceedings of the National Academy of Sciences*, *107*(19), 8537–8542. https://doi.org/10.1073/pnas.0912949107

Welander, P. V., Doughty, D. M., Wu, C.-H., Mehay, S., Summons, R. E., & Newman, D. K. (2012). Identification and characterization of Rhodopseudomonas palustris TIE-1 hopanoid biosynthesis mutants: Hopanoid biosynthesis in R. palustris TIE-1. *Geobiology*, *10*(2), 163–177. https://doi.org/10.1111/j.1472-4669.2011.00314.x

Welander, P. V., Hunter, R. C., Zhang, L., Sessions, A. L., Summons, R. E., & Newman, D. K. (2009). *Hopanoids Play a Role in Membrane Integrity and pH Homeostasis in Rhodopseudomonas palustris TIE-1 ∺ †*. *191*(19), 6145–6156. https://doi.org/10.1128/JB.00460-09

Welander, P. V., & Summons, R. E. (2012). Discovery, taxonomic distribution, and phenotypic characterization of a gene required for 3-methylhopanoid production. *Proceedings of the National Academy of Sciences*, *109*(32), 12905–12910. https://doi.org/10.1073/pnas.1208255109

Wendt, K. U. (2005). Enzyme Mechanisms for Triterpene Cyclization: New Pieces of the Puzzle. *Angewandte Chemie International Edition*, *44*(26), 3966–3971. https://doi.org/10.1002/anie.200500804

Wendt, K. U., Lenhart, A., & Schulz, G. E. (1999). The structure of the membrane protein squalene-hopene cyclase at 2.0 Å resolution. *Journal of Molecular Biology*, *286*(1), 175–187. https://doi.org/10.1006/jmbi.1998.2470

Xu, R., Fazio, G. C., & Matsuda, S. P. T. (2004). On the origins of triterpenoid skeletal diversity. *Phytochemistry*, *65*(3), 261–291. https://doi.org/10.1016/j.phytochem.2003.11.014

Xu, X., & London, E. (2000). The Effect of Sterol Structure on Membrane Lipid Domains Reveals How Cholesterol Can Induce Lipid Domain Formation. *Biochemistry*, *39*(5), 843–849. https://doi.org/10.1021/bi992543v

Yang, Z., & Dos Reis, M. (2011). Statistical properties of the branch-site test of positive selection. *Molecular Biology and Evolution*, *28*(3), 1217–1228. https://doi.org/10.1093/molbev/msq303

Zhai, L., Bonds, A. C., Smith, C. A., Oo, H., Chou, J. C.-C., Welander, P. V., & Dassama, L. M. K. (2023). *Novel sterol binding domains in bacteria* (p. 2022.05.15.491920). bioRxiv. https://doi.org/10.1101/2022.05.15.491920

Zhang, Q., Yu, Y., Vélasquez, J. E., & van der Donk, W. A. (2012). Evolution of lanthipeptide synthetases. *Proceedings of the National Academy of Sciences*, *109*(45), 18361–18366. https://doi.org/10.1073/pnas.1210393109

1047